DAFTAR PUSTAKA

ABBASI, M., ABDOLLAHZADEH, A., OMIDVAR, H., BAGHERI, B. & REZAEI, M. 2016. Incorporation of SiC particles in FS welded zone of AZ31 Mg alloy to improve the mechanical properties and corrosion resistance. *International Journal of Materials Research,* 107**,** 566-572.

ABBASI, M., BAGHERI, B. & SHARIFI, F. 2021. Simulation and experimental study of dynamic recrystallization process during friction stir vibration welding of magnesium alloys. *Transactions of Nonferrous Metals Society of China,* 31**,** 2626-2650.

AFRIN, N., CHEN, D. L., CAO, X. & JAHAZI, M. 2008. Microstructure and tensile properties of friction stir welded AZ31B magnesium alloy. *Materials Science and Engineering: A,* 472**,** 179-186.

AHMED, M. M. Z., EL-SAYED SELEMAN, M. M., AHMED, E., REYAD, H. A., TOUILEB, K. & ALBAIJAN, I. 2022. Friction Stir Spot Welding of Different Thickness Sheets of Aluminum Alloy AA6082-T6. *Materials,* 15**,** 2971.

ARORA, A., DE, A. & DEBROY, T. 2011. Toward optimum friction stir welding tool shoulder diameter. *Scripta materialia,* 64**,** 9-12.

ATAK, A., ŞıK, A. & ÖZDEMIR, V. 2018. Thermo-mechanical modeling of friction stir spot welding and numerical solution with the finite element method. *Int. J. Eng. Appl. Sci,* 5**,** 70-75.

AVEDESIAN, M. M. & BAKER, H. 1999. *ASM specialty handbook: magnesium and magnesium alloys,* ASM international.

AVULA, D., SINGH, R. K. R., DWIVEDI, D. K. & MEHTA, N. K. 2011. Effect of friction stir welding on microstructural and mechanical properties of copper alloy. *World Academy of Science, Engineering and Technology,* 74**,** 214-222.

AYUB, S., GUAN, B. H., AHMAD, F., JAVED, M. F., MOSAVI, A. & FELDE, I. 2021. Preparation Methods for Graphene Metal and Polymer Based Composites for EMI Shielding Materials: State of the Art Review of the Conventional and Machine Learning Methods. *Metals,* 11**,** 1164.

BADARINARAYAN, H., SHI, Y., LI, X. & OKAMOTO, K. 2009a. Effect of tool geometry on hook formation and static strength of friction stir spot welded aluminum 5754-O sheets. *International Journal of Machine Tools and Manufacture,* 49**,** 814-823.

BADARINARAYAN, H., YANG, Q. & ZHU, S. 2009b. Effect of tool geometry on static strength of friction stir spot-welded aluminum alloy. *International Journal of Machine Tools and Manufacture,* 49**,** 142-148.

BALASUBRAMANIAN, N., MISHRA, R. S. & KRISHNAMURTHY, K. 2011. Process forces during friction stir channeling in an aluminum alloy. *Journal of Materials Processing Technology,* 211**,** 305-311.

BALASUBRAMANIAN, V. 2008. Relationship between base metal properties and friction stir welding process parameters. *Materials Science and Engineering: A,* 480**,** 397-403.

BASKORO, A. S., AMAT, M. A. & WIDIYANTO, M. A. Effect of Tools Geometry and Dwell Time on Mechanical Properties and Macrograph of

Two-Stage Refilled Friction Stir Spot Micro Weld. 2019. EDP Sciences, 02002.

BASKORO, A. S., HADISISWOJO, S., KISWANTO, G., AMAT, M. A. & CHEN, Z. W. 2020. Influence of welding parameters on macrostructural and thermomechanical properties in micro friction stir spot welded under high-speed tool rotation. *The International Journal of Advanced Manufacturing Technology*, 106**,** 163-175.

BASKORO, A. S., HADISISWOJO, S., KISWANTO, G., WINARTO, AMAT, M. A. & CHEN, Z. W. 2019. Influence of welding parameters on macrostructural and thermomechanical properties in micro friction stir spot welded under high-speed tool rotation. *The International Journal of Advanced Manufacturing Technology*.

BASKORO, A. S., KISWANTO, G. & WINARTO, W. Effects of high speed tool rotation in micro friction stir spot welding of aluminum A1100. 2014. Trans Tech Publ, 739-742.

BASKORO, A. S., NUGROHO, A. A., RAHAYU, D., KISWANTO, G. & WINARTO, W. Effects of welding parameters in micro friction stir lap welding of aluminum A1100. 2013. Trans Tech Publ, 356-359.

BASKORO, A. S., NUGROHO, A. A. D., RAHAYU, D., SUWARSONO, KISWANTO, G. & WINARTO, W. 2013. Effects of Welding Parameters in Micro Friction Stir Lap Welding of Aluminum A1100. *Advanced Materials Research*, 789**,** 356-359.

BASKORO, A. S., RIYANTO, A., ARIFARDI, M. F. & RUPAJATI, P. Influence of Tools Diameters and Plunge Depth on Mechanical Properties of Micro Friction Stir Spot Welding Materials A1100. 2020. IOP Publishing, 012008.

BUFFA, G., FRATINI, L. & SHIVPURI, R. 2008. Finite element studies on friction stir welding processes of tailored blanks. *Computers & structures*, 86**,** 181-189.

CAO, X. & JAHAZI, M. 2009. Effect of welding speed on the quality of friction stir welded butt joints of a magnesium alloy. *Materials & design*, 30**,** 2033-2042.

CHEN, Y. C. & NAKATA, K. 2008. Friction stir lap joining aluminum and magnesium alloys. *Scripta materialia*, 58**,** 433-436.

CHEN, Y. C. & NAKATA, K. 2010. Effect of surface states of steel on microstructure and mechanical properties of lap joints of magnesium alloy and steel by friction stir welding. *Science and Technology of Welding and Joining*, 15**,** 293-298.

CUI, S., CHEN, Z. W. & ROBSON, J. D. 2010. A model relating tool torque and its associated power and specific energy to rotation and forward speeds during friction stir welding/processing. *International Journal of Machine Tools and Manufacture*, 50**,** 1023-1030.

DARMADI, D. B., ABDILLAH, F. N. & RAHARJO, R. 2019. Controlling the pressure force to obtain a better quality of aluminum 6061 friction stir welded joint. *Восточно-Европейский журнал передовых технологий***,** 6-10.

DEHGHAN MANSHADI, M., GHASSEMI, M., MOUSAVI, S. M., MOSAVI, A. H. & KOVACS, L. 2021. Predicting the Parameters of Vortex Bladeless

Wind Turbine Using Deep Learning Method of Long Short-Term Memory. *Energies,* 14**,** 4867.

DEWAN, M. W., HUGGETT, D. J., LIAO, T. W., WAHAB, M. A. & OKEIL, A. M. 2016. Prediction of tensile strength of friction stir weld joints with adaptive neuro-fuzzy inference system (ANFIS) and neural network. *Materials & Design,* 92**,** 288-299.

DONG, H., HU, W., DUAN, Y., WANG, X. & DONG, C. 2012. Dissimilar metal joining of aluminum alloy to galvanized steel with Al–Si, Al–Cu, Al–Si–Cu and Zn–Al filler wires. *Journal of Materials Processing Technology,* 212**,** 458-464.

ELATHARASAN, G. & KUMAR, V. S. S. 2013. An experimental analysis and optimization of process parameter on friction stir welding of AA 6061-T6 aluminum alloy using RSM. *Procedia Engineering,* 64**,** 1227-1234.

ESMAEILI, A., GIVI, M. K. B. & RAJANI, H. R. Z. 2011. A metallurgical and mechanical study on dissimilar Friction Stir welding of aluminum 1050 to brass (CuZn30). *Materials Science and Engineering: A,* 528**,** 7093-7102.

ESPARZA, J. A., DAVIS, W. C., TRILLO, E. A. & MURR, L. E. 2002a. Friction-stir welding of magnesium alloy AZ31B. *Journal of materials science letters,* 21**,** 917-920.

ESPARZA, J. A., DAVIS, W. C., TRILLO, E. A. & MURR, L. E. 2002b. Friction-stir welding of magnesium alloy AZ31B. *Journal of materials science letters,* 21**,** 917-920.

ETTER, A. L., BAUDIN, T., FREDJ, N. & PENELLE, R. 2007. Recrystallization mechanisms in 5251 H14 and 5251 O aluminum friction stir welds. *Materials Science and Engineering: A,* 445**,** 94-99.

FELDSTEIN, J. G. 2002. Welding and brazing qualifications. *ASME Boil. Press. Vessel Code,* 2**,** 189-225.

FIROUZDOR, V. & KOU, S. 2009. Al-to-Mg friction stir welding: effect of positions of Al and Mg with respect to the welding tool. *Welding Journal,* 88**,** 213-224.

FIROUZDOR, V. & KOU, S. 2010. Al-to-Mg friction stir welding: effect of material position, travel speed, and rotation speed. *Metallurgical and Materials Transactions A,* 41**,** 2914-2935.

GANGWAR, K. & RAMULU, M. 2018. Friction stir welding of titanium alloys: A review. *Materials & Design,* 141**,** 230-255.

GHARACHEH, M. A., KOKABI, A. H., DANESHI, G. H., SHALCHI, B. & SARRAFI, R. 2006. The influence of the ratio of "rotational speed/traverse speed"(ω/v) on mechanical properties of AZ31 friction stir welds. *International Journal of Machine Tools and Manufacture,* 46**,** 1983-1987.

GULATI, P., SHUKLA, D. K., GUPTA, A., SINGH, M., KUMAR, R. & SINGH, J. P. 2020. Microstructural analysis of friction stir welded Mg AZ31 alloy. *Materials Today: Proceedings,* 26**,** 1145-1150.

HAN, K., OHNUMA, I., OKUDA, K. & KAINUMA, R. 2018. Experimental determination of phase diagram in the Zn-Fe binary system. *Journal of Alloys and Compounds,* 737**,** 490-504.

HE, X., GU, F. & BALL, A. 2014. A review of numerical analysis of friction stir welding. *Progress in Materials Science,* 65**,** 1-66.

HIRANO, S. 2003. Microstructure of dissimilar joint interface of magnesium alloy and aluminum alloy by friction stir welding. *QJJWS,* 21**,** 539-544.

HUANG, Y., MENG, X., ZHANG, Y., CAO, J. & FENG, J. 2017. Micro friction stir welding of ultra-thin Al-6061 sheets. *Journal of Materials Processing Technology,* 250**,** 313-319.

HUSSEIN, S. A. & HADZLEY, A. B. 2015. Characteristics of aluminum-to-steel joint made by friction stir welding: A review. *Materials Today Communications,* 5**,** 32-49.

IRAWAN, Y. S., CHOIRON, M. A. & SUPRAPTO, W. 2021. Tensile Strength and Thermal Cycle Analysis of AA6061 Friction Weld Joints With Different Diameters and Various Friction Times. *Eastern-European Journal of Enterprise Technologies,* 2**,** 110.

KALAKI, A., KETABCHI, M. & ABBASI, M. 2014. Thixo-joining of D2 and M2 tool steels: analysis of microstructure and mechanical properties. *International journal of materials research,* 105**,** 764-769.

KEIVANI, R., BAGHERI, B., SHARIFI, F., KETABCHI, M. & ABBASI, M. 2013. Effects of pin angle and preheating on temperature distribution during friction stir welding operation. *Transactions of Nonferrous Metals Society of China,* 23**,** 2708-2713.

KHAN, M. A., ASLAM, F., JAVED, M. F., ALABDULJABBAR, H. & DEIFALLA, A. F. 2022. New prediction models for the compressive strength and dry-thermal conductivity of bio-composites using novel machine learning algorithms. *Journal of Cleaner Production,* 350**,** 131364.

KHAN, M. A., MEMON, S. A., FAROOQ, F., JAVED, M. F., ASLAM, F. & ALYOUSEF, R. 2021. Compressive strength of fly-ash-based geopolymer concrete by gene expression programming and random forest. *Advances in Civil Engineering,* 2021.

KIM, D., BADARINARAYAN, H., KIM, J. H., KIM, C., OKAMOTO, K., WAGONER, R. H. & CHUNG, K. 2010. Numerical simulation of friction stir butt welding process for AA5083-H18 sheets. *European Journal of Mechanics-A/Solids,* 29**,** 204-215.

KOSTKA, A., COELHO, R. S., DOS SANTOS, J. & PYZALLA, A. R. 2009. Microstructure of friction stir welding of aluminium alloy to magnesium alloy. *Scripta Materialia,* 60**,** 953-956.

KUANG, B., SHEN, Y., CHEN, W., YAO, X., XU, H., GAO, J. & ZHANG, J. 2015. The dissimilar friction stir lap welding of 1A99 Al to pure Cu using Zn as filler metal with “pinless” tool configuration. *Materials & Design,* 68**,** 54-62.

KUMAR, K. & KAILAS, S. V. 2008. The role of friction stir welding tool on material flow and weld formation. *Materials Science and Engineering: A,* 485**,** 367-374.

KUMAR, S. S. & ASHOK, S. D. 2014. Development of acoustic emission and motor current based fuzzy logic model for monitoring weld strength and nugget hardness of FSW joints. *Procedia Engineering,* 97**,** 909-917.

KWON, Y. J., SHIGEMATSU, I. & SAITO, N. 2008. Dissimilar friction stir welding between magnesium and aluminum alloys. *Materials Letters,* 62**,** 3827-3829.

LEE, C.-Y., LEE, W.-B., KIM, J.-W., CHOI, D.-H., YEON, Y.-M. & JUNG, S.-B. 2008. Lap joint properties of FSWed dissimilar formed 5052 Al and 6061 Al alloys with different thickness. *Journal of Materials Science,* 43**,** 3296-3304.

LEE, W. B., YEON, Y. M. & JUNG, S. B. 2003. Joint properties of friction stir welded AZ31B–H24 magnesium alloy. *Materials Science and Technology,* 19**,** 785-790.

LEITAO, C., LEAL, R. M., RODRIGUES, D. M., LOUREIRO, A. & VILAÇA, P. 2009. Mechanical behaviour of similar and dissimilar AA5182-H111 and AA6016-T4 thin friction stir welds. *Materials & Design,* 30**,** 101-108.

LI, G., ZHOU, L., ZHOU, W., SONG, X. & HUANG, Y. 2019. Influence of dwell time on microstructure evolution and mechanical properties of dissimilar friction stir spot welded aluminum–copper metals. *Journal of Materials Research and Technology,* 8**,** 2613-2624.

LI, P., KHAN, M. A., EL-ZAHAR, E. R., AWAN, H. H., ZAFAR, A., JAVED, M. F., KHAN, M. I., QAYYUM, S., MALIK, M. Y. & WANG, F. 2022. Sustainable use of chemically modified tyre rubber in concrete: Machine learning based novel predictive model. *Chemical Physics Letters***,** 139478.

LIN, Y.-C., LIU, J.-J., LIN, B.-Y., LIN, C.-M. & TSAI, H.-L. 2012. Effects of process parameters on strength of Mg alloy AZ61 friction stir spot welds. *Materials & Design,* 35**,** 350-357.

LIU, L., WANG, H., SONG, G. & YE, J. N. 2007. Microstructure characteristics and mechanical properties of laser weld bonding of magnesium alloy to aluminum alloy. *Journal of materials science,* 42**,** 565-572.

LOHWASSER, D. & CHEN, Z. 2009. *Friction stir welding: From basics to applications,* Elsevier.

LORRAIN, O., FAVIER, V., ZAHROUNI, H. & LAWRJANIEC, D. 2010. Understanding the material flow path of friction stir welding process using unthreaded tools. *Journal of Materials Processing Technology,* 210**,** 603-609.

LUO, X.-L., FENG, J. & ZHANG, H.-H. 2020. A genetic algorithm for astroparticle physics studies. *Computer Physics Communications,* 250**,** 106818.

MA, Z. Y., FENG, A. H., CHEN, D. L. & SHEN, J. 2018. Recent advances in friction stir welding/processing of aluminum alloys: microstructural evolution and mechanical properties. *Critical Reviews in Solid State and Materials Sciences,* 43**,** 269-333.

MAHONEY, M. W., RHODES, C. G., FLINTOFF, J. G., BINGEL, W. H. & SPURLING, R. A. 1998. Properties of friction-stir-welded 7075 T651 aluminum. *Metallurgical and Materials Transactions A,* 29**,** 1955-1964.

MEIABADI, M. S., MORADI, M., KARAMIMOGHADAM, M., ARDABILI, S., BODAGHI, M., SHOKRI, M. & MOSAVI, A. H. 2021. Modeling the producibility of 3D printing in polylactic acid using artificial neural networks and fused filament fabrication. *Polymers,* 13**,** 3219.

MISHRA, R. S. & MA, Z. Y. 2005a. Friction stir welding and processing. *Materials Science and Engineering: R: Reports,* 50**,** 1-78.

MISHRA, R. S. & MA, Z. Y. 2005b. Friction stir welding and processing. *Materials science and engineering: R: reports,* 50**,** 1-78.

MOHAMMADI, J., BEHNAMIAN, Y., MOSTAFAEI, A., IZADI, H., SAEID, T., KOKABI, A. H. & GERLICH, A. P. 2015. Friction stir welding joint of dissimilar materials between AZ31B magnesium and 6061 aluminum alloys: Microstructure studies and mechanical characterizations. *Materials Characterization,* 101**,** 189-207.

MOHAMMADZADEH S, D., KAZEMI, S.-F., MOSAVI, A., NASSERALSHARIATI, E. & TAH, J. H. M. 2019. Prediction of compression index of fine-grained soils using a gene expression programming model. *Infrastructures,* 4**,** 26.

MORDIKE, B. L. & EBERT, T. 2001. Magnesium: properties—applications—potential. *Materials Science and Engineering: A,* 302**,** 37-45.

MUNITZ, A., COTLER, C., STERN, A. & KOHN, G. 2001. Mechanical properties and microstructure of gas tungsten arc welded magnesium AZ91D plates. *Materials science and engineering: A,* 302**,** 68-73.

NANDAN, R., DEBROY, T. & BHADESHIA, H. K. D. H. 2008. Recent advances in friction-stir welding – Process, weldment structure and properties. *Progress in Materials Science,* 53**,** 980-1023.

NI, Y., FU, L. & CHEN, H. Y. 2019. Effects of travel speed on mechanical properties of AA7075-T6 ultra-thin sheet joints fabricated by high rotational speed micro pinless friction stir welding. *Journal of Materials Processing Technology,* 265**,** 63-70.

PAREEK, M., POLAR, A., RUMICHE, F. & INDACOCHEA, J. E. 2007. Metallurgical evaluation of AZ31B-H24 magnesium alloy friction stir welds. *Journal of materials engineering and performance,* 16**,** 655-662.

PENG, Y., GHAHNAVIYEH, M. B., AHMAD, M. N., ABDOLLAHI, A., BAGHERZADEH, S. A., AZIMY, H., MOSAVI, A. & KARIMIPOUR, A. 2021. Analysis of the effect of roughness and concentration of Fe3O4/water nanofluid on the boiling heat transfer using the artificial neural network: An experimental and numerical study. *International Journal of Thermal Sciences,* 163**,** 106863.

QIU, R., IWAMOTO, C. & SATONAKA, S. 2009. Interfacial microstructure and strength of steel/aluminum alloy joints welded by resistance spot welding with cover plate. *Journal of Materials processing technology,* 209**,** 4186-4193.

RAHMI, M. & ABBASI, M. 2017. Friction stir vibration welding process: modified version of friction stir welding process. *The International Journal of Advanced Manufacturing Technology,* 90**,** 141-151.

RAI, R., DE, A., BHADESHIA, H. & DEBROY, T. 2011. friction stir welding tools. *Science and Technology of welding and Joining,* 16**,** 325-342.

RAMACHANDRAN, K. K., MURUGAN, N. & KUMAR, S. S. 2015. Effect of tool axis offset and geometry of tool pin profile on the characteristics of friction stir welded dissimilar joints of aluminum alloy AA5052 and HSLA steel. *Materials Science And Engineering: A,* 639**,** 219-233.

RAO, H. M., JORDON, J. B., BARKEY, M. E., GUO, Y. B., SU, X. & BADARINARAYAN, H. 2013. Influence of structural integrity on fatigue behavior of friction stir spot welded AZ31 Mg alloy. *Materials Science and Engineering: A,* 564**,** 369-380.

RODRIGUES, D. M., LOUREIRO, A., LEITAO, C., LEAL, R. M., CHAPARRO, B. M. & VILAÇA, P. 2009. Influence of friction stir welding parameters on the microstructural and mechanical properties of AA 6016-T4 thin welds. *Materials & Design,* 30**,** 1913-1921.

SAEID, T., ABDOLLAH-ZADEH, A., SHIBAYANAGI, T., IKEUCHI, K. & ASSADI, H. 2010. On the formation of grain structure during friction stir welding of duplex stainless steel. *Materials Science and Engineering: A,* 527**,** 6484-6488.

SALARI, M. 2020. Dissimilar Friction Stir Welding between Magnesium and Aluminum Alloys. *Journal of Modern Processes in Manufacturing and Production,* 9**,** 65-72.

SALVATI, E., EVERAERTS, J., KAGEYAMA, K. & KORSUNSKY, A. M. 2019. Transverse fatigue behaviour and residual stress analyses of double sided FSW aluminium alloy joints. *Fatigue & Fracture of Engineering Materials & Structures,* 42**,** 1980-1990.

SANCHEZ-TEMBLEQUE, V., VEDIA, V., FRAILE, L. M., RITT, S. & UDIAS, J. M. 2019. Optimizing time-pickup algorithms in radiation detectors with a genetic algorithm.

SATO, Y. S., PARK, S. H. C., MICHIUCHI, M. & KOKAWA, H. 2004. Constitutional liquation during dissimilar friction stir welding of Al and Mg alloys. *Scripta Materialia,* 50**,** 1233-1236.

SCIALPI, A., DE FILIPPIS, L. A. C., CUOMO, P. & DI SUMMA, P. 2008. Micro friction stir welding of 2024–6082 aluminium alloys. *Welding International,* 22**,** 16-22.

SEMUEL, B. M., ONNY, S. S., HAIRUL, A., MUHAMMAD, S. & AGUS, W. 2022. Indentifying the effect of micro friction stir spot welding (μFSSW) parameters on weld geometry, mechanical properties, and metallography on dissimilar materials of AZ31B and AA1100. *Eastern-European Journal of Enterprise Technologies,* 4**,** 13-21.

SEN, M., SHANKAR, S. & CHATTOPADHYAYA, S. 2020. Micro-friction stir welding (μFSW)–A review. *Materials Today: Proceedings,* 27**,** 2469-2473.

SENTHILKUMAR, G., MAYAVAN, T. & MANIKANDAN, H. 2022. Prediction of mechanical characteristics of friction welded dissimilar EN 10028P 355 GH steel and AISI 430 steel joint by fuzzy logic analysis. *Materials Today: Proceedings*.

SENTHILKUMAR, G. & RAMAKRISHNAN, R. 2021. Design of Optimal Parameter for Solid-State Welding of EN 10028-P355 GH Steel Using gray Incidence Reinforced Response Surface Methodology. *Arabian Journal for Science and Engineering,* 46**,** 2613-2628.

SEVVEL, P. & JAIGANESH, V. Improving the mechanical properties of friction stir welded AZ31B magnesium alloy flat plates through axial force investigation. 2014. Trans Tech Publ, 11-14.

SHEHABELDEEN, T. A., ABD ELAZIZ, M., ELSHEIKH, A. H. & ZHOU, J. 2019. Modeling of friction stir welding process using adaptive neuro-fuzzy inference system integrated with harris hawks optimizer. *Journal of Materials Research and Technology,* 8**,** 5882-5892.

SINGARAPU, U., ADEPU, K. & ARUMALLE, S. R. 2015. Influence of tool material and rotational speed on mechanical properties of friction stir welded AZ31B magnesium alloy. *Journal of Magnesium and Alloys,* 3**,** 335-344.

SONG, Y., YANG, X., CUI, L., HOU, X., SHEN, Z. & XU, Y. 2014. Defect features and mechanical properties of friction stir lap welded dissimilar AA2024–AA7075 aluminum alloy sheets. *Materials & Design,* 55**,** 9-18.

SU, C. W., LU, L. & LAI, M. O. 2008. Recrystallization and grain growth of deformed magnesium alloy. *Philosophical Magazine,* 88**,** 181-200.

TABAN, E., GOULD, J. E. & LIPPOLD, J. C. 2010. Dissimilar friction welding of 6061-T6 aluminum and AISI 1018 steel: Properties and microstructural characterization. *Materials & Design (1980-2015),* 31**,** 2305-2311.

THOMAS, W., NICHOLAS, E. D., STAINES, D., TUBBY, P. J. & GITTOS, M. F. 2005. FSW process variants and mechanical properties. *Welding in the World,* 49**,** 4-11.

THOMAS, W. M. & NICHOLAS, E. D. 1997. Friction stir welding for the transportation industries. *Materials & design,* 18**,** 269-273.

THOMAS, W. M., NICHOLAS, E. D., NEEDHAM, J. C., MURCH, M. G., TEMPLE-SMITH, P. & DAWES, C. J. 1995. Friction welding. Google Patents.

THOMAS, W. M., NICHOLAS, E. D., NEEDHAM, J. C., MURCH, M. G., TEMPLESMITH, P. & DAWES, C. J. 1991. Friction stir welding. International Patent Application No. PCT/GB92/02203 and GB Patent Application No. 9125978.8. *US Patent***,** 460-317.

THREADGILL 1997. *Friction stir welds in aluminium alloys – preliminary microstructural assessment.*, TWI Bulletin.

THREADGILL, P. L., LEONARD, A. J., SHERCLIFF, H. R. & WITHERS, P. J. 2009. Friction stir welding of aluminium alloys. *International Materials Reviews,* 54**,** 49-93.

TIER, M. D., ROSENDO, T. S., DOS SANTOS, J. F., HUBER, N., MAZZAFERRO, J. A., MAZZAFERRO, C. P. & STROHAECKER, T. R. 2013. The influence of refill FSSW parameters on the microstructure and shear strength of 5042 aluminium welds. *Journal of materials processing technology,* 213**,** 997-1005.

TOZAKI, Y., UEMATSU, Y. & TOKAJI, K. 2007. Effect of tool geometry on microstructure and static strength in friction stir spot welded aluminium alloys. *International Journal of Machine Tools and Manufacture,* 47**,** 2230-2236.

TRAN, V. X., PAN, J. & PAN, T. 2009. Effects of processing time on strengths and failure modes of dissimilar spot friction welds between aluminum 5754-O and 7075-T6 sheets. *Journal of materials processing technology,* 209**,** 3724-3739.

TUTAR, M., AYDIN, H., YUCE, C., YAVUZ, N. & BAYRAM, A. 2014. The optimisation of process parameters for friction stir spot-welded AA3003-H12 aluminium alloy using a Taguchi orthogonal array. *Materials & Design,* 63**,** 789-797.

UGENDER, S., KUMAR, A. & REDDY, A. S. 2014. Microstructure and mechanical properties of AZ31B magnesium alloy by friction stir welding. *Procedia materials science,* 6**,** 1600-1609.

W.M.THOMAS, E. D. N., J.C. NEEDHAM, M.G.MURCH, P. TEMPLE-SMITH, C.J DAWES. 1991. *Friction stir butt welding*. 9125978· 8.

WANG, K., KHAN, H. A., LI, Z., LYU, S. & LI, J. 2018. Micro friction stir welding of multilayer aluminum alloy sheets. *Journal of Materials Processing Technology,* 260**,** 137-145.

WIDYIANTO, A., BASKORO, A. S., KISWANTO, G. & GANESWARA, M. F. G. 2021. Effect of Welding Sequence and Welding Current on Distortion, Mechanical Properties and Metallurgical Observations of Orbital Pipe Welding on SS 316L. *Eastern-European Journal of Enterprise Technologies,* 2**,** 110.

WIEDENHOFT, A. G., AMORIM, H. J. D., ROSENDO, T. D. S., TIER, M. A. D. & REGULY, A. 2018. Effect of heat input on the mechanical behaviour of Al-Cu FSW lap joints. *Materials Research,* 21.

WOO, W., UNGÁR, T., FENG, Z., KENIK, E. & CLAUSEN, B. 2010. X-ray and neutron diffraction measurements of dislocation density and subgrain size in a friction-stir-welded aluminum alloy.

XUNHONG, W. & KUAISHE, W. 2006. Microstructure and properties of friction stir butt-welded AZ31 magnesium alloy. *Materials Science and Engineering: A,* 431**,** 114-117.

YAN, F., ZHANG, Y., SHEN, J., FU, X. & MI, S. 2021. A new calculation method of viscoplastic heat production generated by plastic flow of friction stir welding process. *Materials Chemistry and Physics,* 270**,** 124795.

YANG, J., CHEN, J., ZHAO, W., ZHANG, P., YU, Z., LI, Y., ZENG, Z. & ZHOU, N. 2018. Diode laser welding/brazing of aluminum alloy to steel using a nickel coating. *Applied Sciences,* 8**,** 922.

YANG, Q., MIRONOV, S., SATO, Y. S. & OKAMOTO, K. 2010. Material flow during friction stir spot welding. *Materials Science and Engineering: A,* 527**,** 4389-4398.

YANG, X.-W., FENG, W.-Y., LI, W.-Y., DONG, X.-R., XU, Y.-X., QIANG, C. H. U. & YAO, S.-T. 2019. Microstructure and properties of probeless friction stir spot welding of AZ31 magnesium alloy joints. *Transactions of Nonferrous Metals Society of China,* 29**,** 2300-2309.

YIN, Y. H., SUN, N., NORTH, T. H. & HU, S. S. 2010. Hook formation and mechanical properties in AZ31 friction stir spot welds. *Journal of Materials Processing Technology,* 210**,** 2062-2070.

ZHANG, H., LIN, S. B., WU, L., FENG, J. C. & MA, S. L. 2006. Defects formation procedure and mathematic model for defect free friction stir welding of magnesium alloy. *Materials & design,* 27**,** 805-809.

ZHANG, H., WU, H., HUANG, J., SANBAO, L. I. N. & LIN, W. U. 2007. Effect of welding speed on the material flow patterns in friction stir welding of AZ31 magnesium alloy. *Rare Metals,* 26**,** 158-162.

ZHANG, Z., LIU, Y. L. & CHEN, J. T. 2009. Effect of shoulder size on the temperature rise and the material deformation in friction stir welding. *The International Journal of Advanced Manufacturing Technology,* 45**,** 889.

ZHANG, Z., YANG, X., ZHANG, J., ZHOU, G., XU, X. & ZOU, B. 2011. Effect of welding parameters on microstructure and mechanical properties of friction stir spot welded 5052 aluminum alloy. *Materials & Design,* 32**,** 4461-4470.

LAMPIRAN

LAMPIRAN 1. Sertifikat Sebagai Presenter dalam ISAIME Conference

CERTIFICATE OF PRESENTER

The certificate presented to :

SEMUEL BORON MEMBALA

Has participated with a paper entitled

Variation of Micro Friction Stir Spot Welding (mFSSW) Parameters on Metallography With Similar Materials AA1100

At *The International Symposium on Advance and Innovation in Mechanical Engineering* (ISAIME) 2022
held on October 13 , 2022 by Mechanical Engineering Departement of Universitas Hasanuddin in collaboration with
Badan Kerja Sama Teknik Mesin Indonesia (BKS-TM Indonesia)

Makassar, October 13 , 2022

ORGANIZING COMMITTEE
ISAIME 2022

Dr. Eng. Novriany Amaliyah, ST., MT.
Organizing Commite ISAIME 2022

Lampiran 2. Data-data penelitian µFSSW pada *dissimilar material* AA1100-AZ31B

1. Geometri las

Tabel 29. Hasil uji geometri las pada *dissimilar material* AA1100-AZ31B

			Pengujian 1				Pengujian 2			
No	DT	PD	Pin Diameter (mm)	Shoulder Diameter (mm)	*Plunge depth* (mikron)	TMAZ Area (mm^2)	Pin Diameter (mm)	Shoulder Diameter (mm)	*Plunge depth* (mikron)	TMAZ Area (mm^2)
1	300	400	2,389	4,109	0,27	5,028	2,434	4,157	0,34	5,229
2	300	500	2,489	4,185	0,51	5,141	2,46	4,554	0,53	6,898
3	300	600	2,535	4,114	0,57	6,682	2,457	4,756	0,55	7,012
4	500	400	2,46	4,554	0,37	6,898	2,425	4,185	0,38	5,141
5	500	500	2,501	4,498	0,44	8,193	2,482	4,588	0,47	8,09
6	500	600	2,491	4,466	0,61	7,791	2,569	4,667	0,59	8,95
7	700	400	2,457	4,756	0,41	7,012	2,535	4,114	0,44	6,682
8	700	500	2,589	4,667	0,54	8,95	2,491	4,466	0,5	7,791
9	700	600	2,646	4,861	0,64	9,357	2,494	4,682	0,59	9,195

Tabel 30. Hasil rata-rata uji geometri las pada *dissimilar material* AA1100-AZ31B

No	DT	PD	Pin Diameter (mm)	Error Pin diameter	SD	Shoulder Diameter (mm)	Error shoulder diameter	SD
1	300	400	2,41	5,06%	0,03	4,13	16,57%	0,03
2	300	500	2,47	2,58%	0,02	4,37	11,80%	0,26
3	300	600	2,50	1,73%	0,06	4,44	10,48%	0,45
4	500	400	2,44	3,84%	0,02	4,37	11,80%	0,26
5	500	500	2,49	1,91%	0,01	4,54	8,30%	0,06
6	500	600	2,53	0,39%	0,06	4,57	7,82%	0,14

7	700	400	2,50	1,73%	0,06	4,44	10,48%	0,45
8	700	500	2,54	0,00%	0,07	4,57	7,82%	0,14
9	700	600	2,57	1,18%	0,11	4,77	3,68%	0,13
No	DT	PD	*Plunge depth* (micron)	Error *plunge depth*	SD	TMAZ Area (mm^2)	SD	
1	300	400	305,00	23,75%	49,50	5,13	0,14	
2	300	500	520,00	4,00%	14,14	6,02	1,24	
3	300	600	560,00	6,67%	14,14	6,85	0,23	
4	500	400	375,00	6,25%	7,07	6,02	1,24	
5	500	500	455,00	9,00%	21,21	8,14	0,07	
6	500	600	600,00	0,00%	14,14	8,37	0,82	
7	700	400	425,00	6,25%	21,21	6,85	0,23	
8	700	500	520,00	4,00%	28,28	8,37	0,82	
9	700	600	615,00	2,50%	35,36	9,28	0,11	

2. Kekuatan tarik geser dan silang

Tabel 31. Hasil pengujian kekuatan tarik geser pada *dissimilar material* AA1100-AZ31B

			Pengujian 1	Pengujian 2	Rata-rata	
No	DT	PD	Max shear load (N)	Max shear load (N)	Max shear load (N)	SD
1	300	400	245,274	229,130	237,20	8,07
2	300	500	361,689	359,347	360,52	1,17
3	300	600	361,944	367,986	364,97	3,02
4	500	400	312,036	332,378	322,21	10,17
5	500	500	374,060	347,565	360,81	13,25
6	500	600	359,742	371,460	365,60	5,86

7	700	400	382,486	369,209	375,85	6,64
8	700	500	398,900	375,275	387,09	11,81
9	700	600	373,376	381,285	377,33	3,95

Tabel 32. Hasil pengujian kekuatan tarik silang pada *dissimilar material* AA1100-AZ31B

			Pengujian 1	Pengujian 2	Rata-rata	
No	DT	PD	Max cross load (N)	Max cross load (N)	Max cross load (N)	SD
1	300	400	21,620	19,237	20,43	1,19
2	300	500	20,982	23,085	22,03	1,05
3	300	600	24,697	23,127	23,91	0,79
4	500	400	22,761	24,732	23,75	0,99
5	500	500	25,078	28,573	26,83	1,75
6	500	600	25,717	28,247	26,98	1,27
7	700	400	25,954	27,975	26,96	1,01
8	700	500	26,659	29,745	28,20	1,54
9	700	600	27,838	31,375	29,61	1,77

3. Tegangan (*stress*)

Tabel 33. Hasil perhitungan tegangan geser pada *dissimilar material* AA1100-AZ31B

			Pengujian 1				Pengujian 2				Rata-rata	
No	DT	PD	Max shear load (N)	Diameter nugget (mm)	Luas area (mm^2)	Tegangan (N/mm^2)	Max shear load (N)	Diameter nugget (mm)	Luas area (mm^2)	Tegangan (N/mm^2)	Tegangan (N/mm^2)	SD
1	300	400	245,274	4,109	13,261	18,497	229,130	4,157	13,572	16,882	17,69	1,14
2	300	500	361,689	4,185	13,756	26,294	359,347	4,554	16,288	22,062	24,18	2,99
3	300	600	361,944	4,114	13,293	27,228	367,986	4,756	17,765	20,714	23,97	4,61
4	500	400	312,036	4,554	16,288	19,157	332,378	4,185	13,756	24,163	21,66	3,54
5	500	500	374,060	4,498	15,890	23,540	347,565	4,588	16,532	21,023	22,28	1,78
6	500	600	359,742	4,466	15,665	22,965	371,460	4,667	17,107	21,714	22,34	0,88
7	700	400	382,486	4,756	17,765	21,530	369,209	4,114	13,293	27,775	24,65	4,42
8	700	500	398,900	4,667	17,107	23,318	375,275	4,466	15,665	23,956	23,64	0,45
9	700	600	373,376	4,861	18,558	20,119	381,285	4,682	17,217	22,146	21,13	1,43

Tabel 34. Hasil perhitungan tegangan silang pada *dissimilar material* AA1100-AZ31B

			Pengujian 1				Pengujian 2				Rata-rata	
No	DT	PD	Max cross load (N)	Diameter nugget (mm)	Luas area (mm^2)	Tegangan (N/mm^2)	Max cross load (N)	Diameter nugget (mm)	Luas area (mm^2)	Tegangan (N/mm^2)	Tegangan (N/mm^2)	SD
1	300	400	21,620	4,109	13,261	1,630	19,237	4,157	13,572	1,417	1,52	0,15
2	300	500	20,982	4,185	13,756	1,525	23,085	4,554	16,288	1,417	1,47	0,08
3	300	600	24,697	4,114	13,293	1,858	23,127	4,756	17,765	1,302	1,58	0,39
4	500	400	22,761	4,554	16,288	1,397	24,732	4,185	13,756	1,798	1,60	0,28

5	500	500	25,078	4,498	15,890	1,578	28,573	4,588	16,532	1,728	1,65	0,11
6	500	600	25,717	4,466	15,665	1,642	28,247	4,667	17,107	1,651	1,65	0,01
7	700	400	25,954	4,756	17,765	1,461	27,975	4,114	13,293	2,105	1,78	0,46
8	700	500	26,659	4,667	17,107	1,558	29,745	4,466	15,665	1,899	1,73	0,24
9	700	600	27,838	4,861	18,558	1,500	31,375	4,682	17,217	1,822	1,66	0,23

4. Masukan panas (*heat input*)

Tabel 35. Hasil perhitungan masukan panas pada *dissimilar material* AA1100-AZ31B

DT (ms)	PD (micron)	Max. Heat Input (kJ)
300	400	11,287
300	500	11,317
300	600	15,506
500	400	20,204
500	500	27,488
500	600	22,957
700	400	31,083
700	500	29,464
700	600	35,346

5. *Microhardness*

Tabel 36. Hasil pengujian *microhardness* pada *dissimilar material* AA1100-AZ31B

Pengujian 1		
Posisi	Nilai kekerasan (HV)	Zona
1	28	HAZ
2	58	SZ
3	154	SZ
4	63	SZ
5	30	HAZ
6	52	HAZ
7	57	SZ
8	53	SZ
9	55	SZ
10	51	HAZ

Pengujian 2		
Posisi	Nilai kekerasan (HV)	Zona
1	30	HAZ
2	68	SZ
3	203	SZ
4	61	SZ
5	34	HAZ
6	55	HAZ
7	60	SZ
8	57	SZ
9	63	SZ
10	53	HAZ

Pengujian 3		
Posisi	Nilai kekerasan (HV)	Zona
1	33	HAZ
2	79	SZ
3	213	SZ
4	80	SZ
5	36	HAZ
6	58	HAZ
7	68	SZ
8	65	SZ
9	72	SZ
10	60	HAZ

Lampiran 3. Artikel yang sudah di Pulikasi

1. Artikel 1 (Published di Eastern-European Journal of Enterprise Technologies)

Micro-friction stir spot welding (μFSSW) is one type of welding that is suitable for joining lightweight materials. One of the challenges in joining lightweight materials with μFSSW is that the material is easily perforated, or the join is not strong enough, so it is necessary to select the right μFSSW parameters. In this article discusses about investigates the micro-Friction Stir Spot Welding (μFSSW) parameters on weld geometry, mechanical properties, and metallography on dissimilar materials of AZ31B and AA1100. The material thickness of the AZ31B and AA100 is 0.5 mm and 0.32 mm, respectively. The μFSSW tool is made of high-speed steel (HSS) with a pin diameter of 0.25 mm and a shoulder diameter of 0.5 mm. The constant process parameters of the μFSSW joint used, i. e., plunge depth, dwell time plunge rate, and high tool rotational speed of 33,000 rpm. Welding test results include weld geometry, mechanical properties, and metallography. Weld geometry testing to determine the weld nugget diameter. The mechanical properties test was shear tensile test and cross tensile test, while the metallographic test included macrostructure and microstructure observations. The results of the FSSW weld geometry show that at a dwell time of 700 milliseconds and a plunge depth of 600 microns, the weld pin diameter and weld shoulder diameter are close to the pin diameter and the diameter of the shoulder tool used. Dwell time and plunge depth has a significant effect on tensile strength. The maximum shear and cross loads achieved were 387±17 N and 29±2 N, respectively. Intermetallic compounds (IMC) are observed at the interface of the two materials, while a dwell time of 700 milliseconds give the effect of cracks on the inside of the weld

Keywords: micro-Friction Stir Spot Welding (μFSSW), dissimilar material, AA1100, AZ31B

UDC 621
DOI: 10.15587/1729-4061.2022.263350

INDENTIFYING THE EFFECT OF MICRO FRICTION STIR SPOT WELDING (μFSSW) PARAMETERS ON WELD GEOMETRY, MECHANICAL PROPERTIES, AND METALLOGRAPHY ON DISSIMILAR MATERIALS OF AZ31B AND AA1100

Semuel Boron Membala
Doctoral Student*
Onny Sutyono Sutresman
Doctorate, Professor*
Hairul Arsyad
Corresponding author
Doctorate, Assistant Professor*
Muhammad Syahid
Doctorate, Assistant Professor*
Agus Widyianto
Doctorate, Head of Autobody Workshop and Painting Laboratory
Department of Automotive Engineering Education
Faculty of Engineering
Universitas Negeri Yogyakarta
Jl. Colombo No. 1, Karang Gayam, Caturtunggal, Kec. Depok, Kabupaten Sleman, Daerah Istimewa Yogyakarta, Indonesia, 55281
E-mail: aguswidyianto@uny.ac.id
*Departement of Mechanical Engineering
Faculty of Engineering
Hasanuddin University
Jl. Poros Malino KM., 6, Bontomarannu Gowa, Sulawesi Selatan, Indonesia, 92171

Received date 21.06.2022
Accepted date 18.08.2022
Published date 26.08.2022

How to Cite: *Membala, S. B., Suresman, O. S., Arsyad, H., Syahid, M., Widyianto, A. (2022). Indentifying the effect of micro friction stir spot welding (μFSSW) parameters on weld geometry, mechanical properties, and metallography on dissimilar materials of AZ31B and AA1100. Eastern-European Journal of Enterprise Technologies, 4 (12 (118)), 13–21. doi: https://doi.org/10.15587/1729-4061.2022.263350*

1. Introduction

Lightweight materials often used as structural materials for manufacturing a vehicle are aluminum alloys and magnesium alloys. The properties of aluminum alloys include lightweight materials, high strength, and easy to form. In comparison, the properties of magnesium alloys include having a lower density than aluminum alloys and being the lightest material for structural materials. Combining these two materials is a promising alloy if appropriately manufactured for structural materials in automotive applications [1]. Several researchers have carried out various welding technologies to unite these two materials. Liquid-state welding is considered less suitable for welding these two materials because it can damage the mechanical properties, solidification cracks, high residual stresses, and high levels of intermetallic compounds in the weld [2, 3].

The FSW process is widely used for its excellent strength and ductility and for minimizing residual stresses and warp-

ing of base metals. FSW has been recognized as the most important development of metal welding technology in 10 years and is a "green technology" due to its energy efficiency, environmental friendliness, and versatility. Compared to traditional welding processes, FSW consumes much less energy. In addition, this is an environmentally friendly process as it does not use any inert gas or flux. So far, the process of welding aluminum with a thickness of less than 1,000 μm is still under development [4].

Using inappropriate parameters in the Micro Friction Stir Weld (μFSW) welding process may not optimize the mechanical properties, residual stresses, and defects such as: B. Defects of hooks [5]. The friction stir welding process between AA2024 and AA7075 using a lap joint type connection produces voids when the AA2024 series is on the top (front), while the AA7075 series has stronger mechanical properties voids occur at (front). This is not the case. The shear stress in the welded joint increases with increasing welding speed [6]. Friction stir welding (FSW) is superior to fusion welding when welding dissimilar metals. FSW offers many advantages in reducing welding defects such as punching, segregation, cracking, and IMC formation [7]. Due to these attractive advantages, FSW is widely used for welding dissimilar metals [8]. A lot of research has been done on FSW for aluminum and steel.

The key to success in FSW welding lies in the tool design, and welding parameters used [9]. In addition, the type of material and thickness are also other factors for the success of FSW welding. The most commonly used material is aluminum. FSW welding on aluminum material with a thickness of <1 mm has been successfully carried out using the high-speed tool rotation method [10]. Joining dissimilar materials does have its challenges. First, where must understand each material's mechanical and thermal properties. From several studies related to the joining of dissimilar materials using the FSSW method, it is still relevant to use today. Therefore, the research shown to investigate the welding parameters of FSSW on aluminum and magnesium materials is still relevant.

2. Literature review and problem statement

Friction stir welding (FSW) is solid-state welding that can connect aluminum alloy materials and magnesium alloys well. FSW with the material below 1000 microns is also called Micro Friction Stir Welding (μFSW), which was first discovered by TWI 1991 [9]. FSW has been proven to be able to join several similar materials such as aluminum alloys [10, 11], steel alloy [12], magnesium [13], copper [14] dan titanium [15]. Paper [10] reports on using FSSW to weld aluminum materials with a thickness of less than 1 mm. FSSW welding parameters such as plunge rate and dwell time are investigated for their effect on weld quality. The results showed that the dwell time did not significantly influence the maximum temperature in the center of the weld. However, the plunge rate affects the material's hardening and softening.

The steel alloy material can also be connected using FSSW. The paper [12] examines microstructure evolution after the FSSW welding process. The results showed that the Stir Zone (SZ) area had a finer grain size than other areas. Subsequent research used AZ61 magnesium material with a thickness of >1 mm [13]. The varied FSSW welding parameters are rotational speed and dwell time tools to see their effect on mechanical and microstructure properties. Increasing the dwell time can improve its mechanical properties while the grain size formed in the SZ area is always small.

In addition, FSW is also effective for welding dissimilar materials such as Mg/Al [1], Al/steel [16], Mg/steel [17], Al/Cu [18] dan Al/brass [19]. The joining of dissimilar materials between Al 6061 and AZ31B has been successfully carried out with a thickness of >1 mm with the formation of intermetallic compounds (IMCs) in the weld zone [1]. Another study between magnesium and steel coupled with zinc between the two materials can improve weldability and quality [17]. FSSW is also effective for joining different materials between aluminum and steel. From several journal reviews [16], it is stated that there are at least three techniques that can be used to connect Al-steel with FSSW, including the annealing technique, plunging technique, and diffusion technique. Other FSSW studies using different materials are aluminum and copper [18]. This study's results indicate the presence of IMCs at the interface of the two materials. In addition, increasing the dwell time can increase the heat input while the hardness value increases in the SZ area.

Several researchers have conducted several studies on dissimilar materials between aluminum and magnesium [1, 20]. The paper [21] reported that intermetallic compounds (IMC) were formed between the surfaces of the two materials, increased welded joints, and decreased weld cracking occurred at low tool speeds. Lap joints are often used for FSW, where the tensile strength of the welded joint increases with increasing tool rotation and travel speeds [1]. In other research [22] used AZ31B-O and A5052P-O materials, where rotation speeds of 1000 rpm produce a maximum tensile strength of 132 MPa.

The paper [23] presents the results of research friction stir spot welding of AZ31 to microstructure and mechanical properties. Shown, that the rotation speed and residence time are increased, the depth of the stirring zone gradually increases. Defects in the hook extend from the interface between the two plates to the surface of the top plate. But there are unresolved problems related to mechanical properties which are still low. The reasons for this may be (objective difficulties related to rotational speed and tool dimensions and tool materials which make relevant research impractical, etc.). The way to overcome these difficulties can be done by using a higher tool rotation speed and a variety of FSSW welding parameters. This approach is used in [10] but the material used in this study is aluminum. All this indicates that it is advisable to carry out a study to investigate the effect of FSSW parameters on dissimilar materials between AZ31B and AA1100.

Many researches on micro Friction Stir Welding (μFSW) has been carried out for similar materials such as aluminum alloys [10]. There are several parameters to consider in μFSW, such as tool geometry, tool rotation, travel speeds, and downward force [23]. However, from several studies that have been carried out, μFSW research on spot joints with dissimilar materials between magnesium and aluminum has not been widely carried out. So, this study aims to determine the effect of micro-Friction Stir Spot Welding (μFSSW) process parameters on weld geometry, mechanical properties, and metallography of aluminum and magnesium alloys with high tool rotation speed. Weld geometry is indicated by the diameter of the weld nugget and the penetration depth, while the welded joint's strength indicates the mechanical properties.

Metallographic observations included macrostructural and microstructural tests by a cross-section of the specimen.

3. The aim and objectives of the study

The aim of the study is identifying the effect of micro-Friction Stir Spot Welding (μFSSW) parameters such as dwell time and plunge depth on weld geometry, mechanical properties, and metallography. This will make it possible to join dissimilar materials between magnesium (AZ31B) and aluminum (AA1100).

To achieve this aim, the following objectives are accomplished:

– to investigate the weld geometry produced after the welding process;

– to investigate the weld's mechanical properties (shear tensile and cross tensile);

– to investigate the macrostructure and microstructure welds results.

4. Material and method of experiment

This study uses dissimilar materials between aluminum AA100 and magnesium AZ31B in micro-Friction Stir Spot Welding (μFSSW) with plate thicknesses of 0.32 mm and 0.5 mm, respectively. Chemical composition tests for AA100 and AZ31B materials have been carried out using an optical emission spectrometer (OES), and the results are shown in Table 1. Before welding, both materials were cleaned using acetone to remove any remaining dirt or dust on the plate surface.

Table 1

Chemical composition (wt %) of AA1100 and AZ31B

AA1100	Al	Zn	Mn	Fe	Si	Cu	Ti	Mg
	99.1	0.070	0.043	0.471	0.109	0.057	0.012	0.019
AZ31B	Al	Zn	Mn	Fe	Si	Cu	Ni	Mg
	3.10	0.99	0.30	0.0029	0.014	0.0009	0.00063	Balance

The welding joint used is spot welding on μFSSW. Specimens were prepared for three tests (shear load, cross tensile load, and metallography) with different dimensions. The dimensions of the specimen for the shear load test are shown in Fig. 1, *a*, with a length of 50 mm and a width of 25 mm. Fig. 1, *b* shows the dimensions of the specimen for the cross tensile load test with a length of 125 mm and a width of 25 mm. Meanwhile, the specimen dimensions in Fig. 1, *c* are 30 mm long and 25 mm wide for metallographic testing. Each test specimen was replicated three time.

The tool used for μFSSW is shown in Fig. 2. The tool material used is made of HSS, which is prepared by turning machining, which has a shoulder diameter of 4.95 mm, pin diameter of 2.54, and pin height of 0.65 mm. The friction stir spot welding machine in this study uses a tensile test machine, a modified result of the EMCO CNC TU-3A milling machine, with an accuracy of 0.01 mm. In contrast, the spindle used comes from a Maktec turner drill machine type MT912 with a die grinder specification of 6 mm, and the spindle rotation speed without load is 33,000 rpm. Table 2 shows the parameters of the μFSSW welding process used in this study.

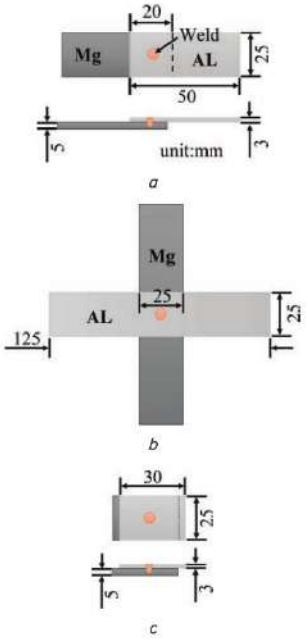

Fig. 1. Dimensions of the specimen for testing: *a* – shear load; *b* – cross tensile load; *c* – metallography

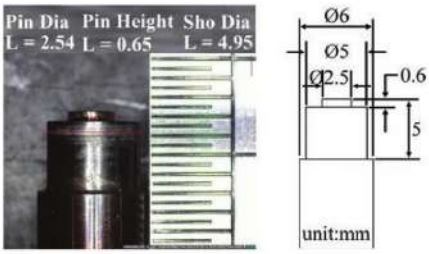

Fig. 2. Dimension tool of micro-Friction Stir Spot Welding

Table 2

Parameter process of μFSSW

No.	Dwell time (milliseconds)	Plunge depth (microns)	Plunge rate (mm/s)
1	300	400	0.4
2	300	500	
3	300	600	
4	500	400	
5	500	500	
6	500	600	
7	700	400	
8	700	500	
9	700	600	

Weld geometry testing is done by measuring the diameter of the weld nugget, the area of Thermo-Mechanically Affected

Zone (TMAZ), and the depth of penetration. Measurement of weld nugget diameter and area of TMAZ using a digital microscope (Dino-Lite AM 4115 Series) while measurement of penetration depth using caliper and caliper attachment. Shear tensile and cross tensile tests were carried out CNC machine A&D tension machine with a capacity of 50 KN using a displacement rate of 0.2 mm/min and 3 mm/min for shear tensile test and cross tensile test, respectively. Metallographic observations were made by cutting the weld crosswise, and then the specimen was mounted with resin. Furthermore, the specimens were sanded to a roughness of 2000 and polished using TiO_2+aceton solution to bring out the microstructure of the welding results using etching with Keller's reagent. The macrostructure was observed using a digital microscope (Dino-Lite AM 4115 Series), while the microstructure was observed using the Oxion Inverso OX 2153-PLM optical microscope.

5. Results of experiment the weld quality of dissimilar material AZ31B-AA1100 using micro-Friction Stir Spot Welding

5. 1. Result of weld geometry

The results of the μFSSW weld are shown in Fig. 3. There are three samples for the test specimen, including shear tensile (Fig. 3, *a*), cross tensile (Fig. 3, *b*), and metallography (Fig. 3, *c*). Each specimen was replicated three times for each parameter variation.

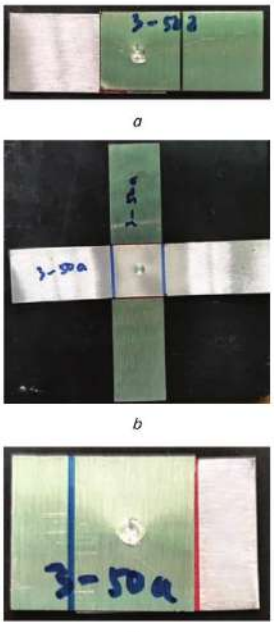

a

b

c

Fig. 3. Micro-Friction Stir Spot Welding weld results for test specimens: *a* – shear tensile; *b* – cross tensile; *c* – metallography

Weld geometry testing on μFSSW can be seen from the nugget diameter (pin diameter and shoulder diameter), measured plunge depth, and TMAZ area. Variations of μFSSW parameters used are dwell time (DT) in milliseconds and plunge depth (PD) in microns. Fig. 4 shows the results of the μFSSW weld on the top view and the measurement of the nugget diameter. At the same time, the results of μFSSW on the back view and TMAZ area measurements are shown in Fig. 5.

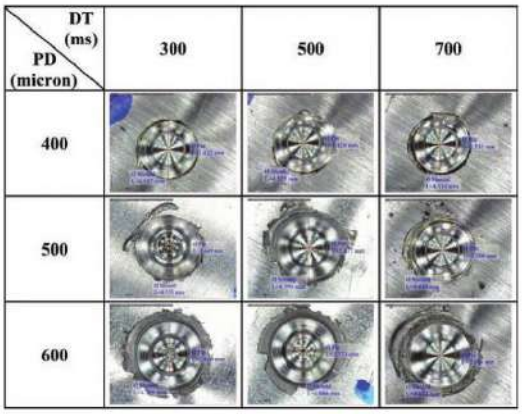

Fig. 4. Weld results from micro-Friction Stir Spot Welding on top view and nugget diameter measurement

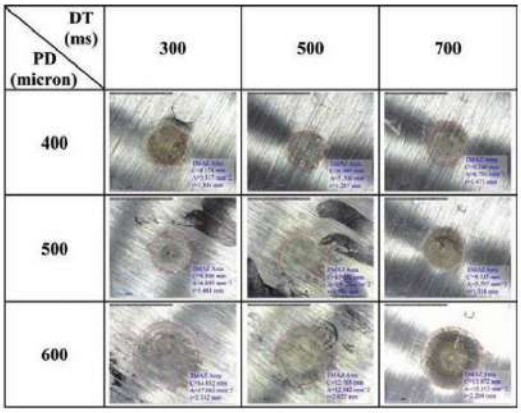

Fig. 5. Welding results from micro-Friction Stir Spot Welding on back view and Thermo-Mechanically Affected Zone area measurement

Visually it can be seen that increasing the plunge depth can widen the diameter of the shoulder. However, increasing the dwell time in welding has no significant effect on the diameter of the nugget. This is due to the height of the pin tool used being 654 microns so if the plunge depth is increased, it will hit the shoulder part of the tool, which has a diameter of 4.954 mm. Adding the plunge depth and dwell time greatly affects the TMAZ area. It can be seen that the longer the

welding takes place, the wider the TMAZ area will be more visible and larger on the back of the weld.

The results of the measurement of the μFSSW weld geometry can be seen in Fig. 6. Fig. 6, *a* shows the results of measuring the diameter of the pin, where there is a trend of increasing the diameter of the pin when increasing the plunge depth and dwell time. The measured pin diameter is close to the diameter of the pin tool used. However, the dwell time of 700 milliseconds produces a weld pin diameter relative to the tool pin diameter. The diameter of the largest welding pin is 2.57 mm with an error of 0.11 % at the dwell time parameter of 700 milliseconds and the plunge depth of 600 microns. This is due to if the welding process lasts longer, it will generate more heat so that it can increase the diameter of the welding pin.

Meanwhile, the measured shoulder diameter is still below the shoulder pin diameter (Fig. 6, *b*). The largest diameter of the weld shoulder is 4.77 mm with an error of 0.13 % at the dwell time parameter of 700 milliseconds and the plunge depth of 600 microns. This is because of the influence of the depth of the plunge used. A low plunge depth will cause the diameter of the shoulder pin not to rub completely against the material so that the diameter of the weld shoulder will be smaller and vice versa. Dwell time and tool geometry have an effect on weld geometry in μFSSW [24]. The weld geometry will be bigger if the dwell time is increased, as well as changing the tool geometry can also increase the weld geometry.

The measured plunge depth with the plunge depth set on the tool shows a difference, especially at a dwell time of 300 milliseconds (Fig. 6, *c*). However, for a dwell time of 700 milliseconds, the result of the measured plunge depth with the plunge depth set in the dial is appropriate. This is because at a dwell time of 300 milliseconds, the heat generated due to friction between the tool and the specimen is still lacking so that the depth of the plunge that is formed is not maximized. It is different from the dwell time of 700 milliseconds, at this dwell time, the heat received by the specimen is higher because the friction that occurs is longer so that the depth of the plunge is maximized. The TMAZ area is influenced by the depth of the plunge and the dwell time, where both parameters have a straight ratio to the TMAZ area (Fig. 6, *d*). The longer the friction between the tool and the specimen, the greater the heat, causing the TMAZ area to increase. This is also supported by the plunge depth that is getting deeper. The area of TMAZ formed from 5.13 mm^2 to 9.28 mm^2, with the largest error being 1.24 %.

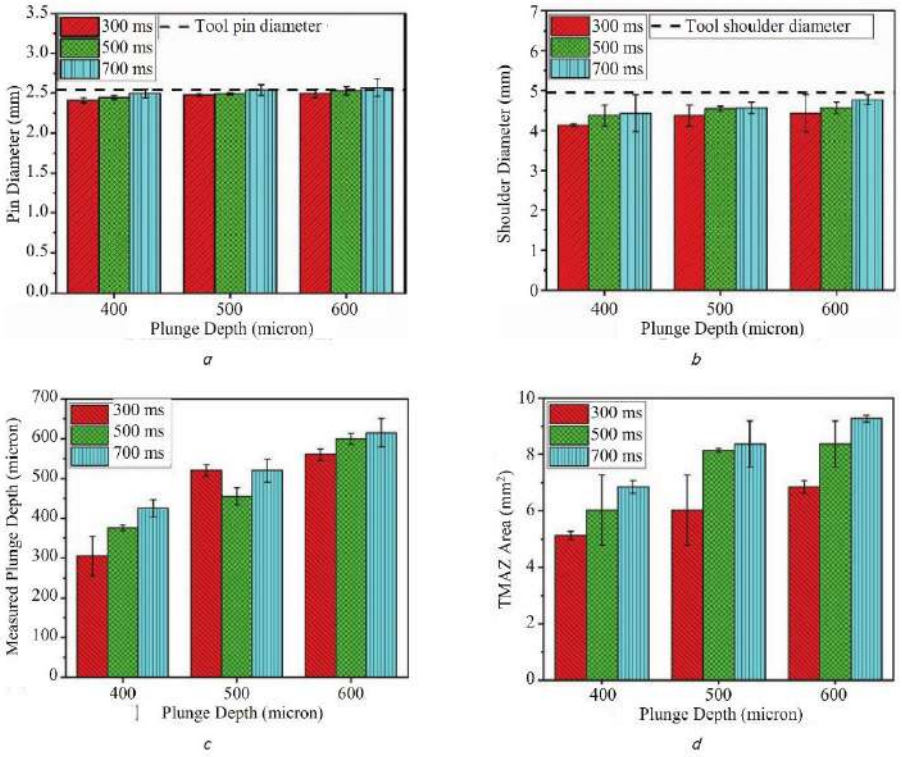

Fig. 6. Weld geometry micro-Friction Stir Spot Welding of: *a* – pin diameter; *b* – shoulder diameter; *c* – measured plunge depth; *d* – thermo-mechanically affected zone area

5. 2. Result of tensile test

Mechanical properties testing carried out is a shear tensile test and cross tensile test. The fracture results from the shear tensile and cross tensile tests are shown in Fig. 7 *a*, *b*, respectively. The results of the tensile test fracture showed a hole in the aluminum specimen. This shows that the joints between dissimilar materials between aluminum and magnesium can be welded using the μFSSW method.

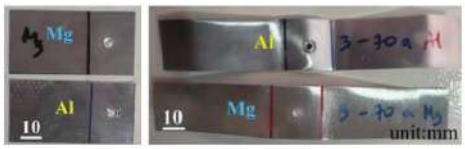

a *b*

Fig. 7. Fracture modes micro-Friction Stir Spot Welding: *a* – shear tensile; *b* – cross tensile

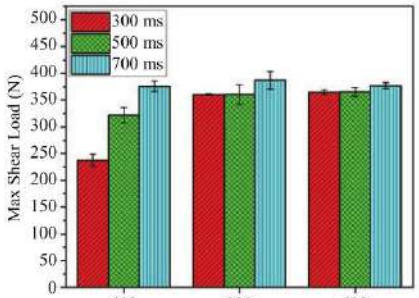

a

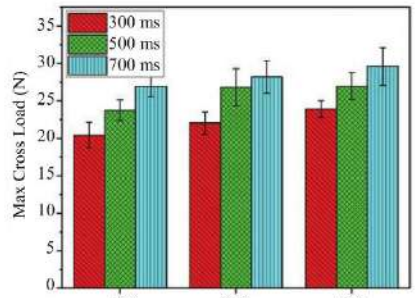

b

Fig. 8. Tensile test micro-Friction Stir Spot Welding of: *a* – max. shear load; *b* – max. cross load

The tensile test resulted in the maximum shear and cross loads shown in Fig. 8, *a*, *b*, respectively. The maximum shear load is 387.09 N at a dwell time of 700 milliseconds and a plunge depth of 500 microns with an error of 16.71 %. In comparison, the dwell time of 700 milliseconds and a plunge depth of 600 microns produce the largest maximum cross load of 29.61 N with an error of 2.50 %. Increasing the plunge depth can increase the maximum load as well as increasing the dwell time can also increase the maximum load of the weld. μFSSW parameters such as dwell time and plunge depth influence the maximum load. By increasing the plunge depth, the joint between the two specimens will be stronger in this case also depending on the thickness of the plate used and the tool. Then the longer the friction between the tool and the specimen will affect the heat and the weld joint's quality [23]. Dwell time does affect the increase in tensile strength [24].

5. 3. Result of metallography

Metallographic testing was carried out on several parameters by cutting the specimen crosswise. Fig. 9 shows the results of metallographic observations at a dwell time of 300 milliseconds and a plunge depth of 600 microns. Aluminum AA100 is placed on the top sheet, while magnesium AZ31B is placed on the bottom sheet. The macrostructural observations are shown in Fig. 9, *a*, which does not show the formation of flashes. However, the plunge depth that is seen still looks very shallow. The dwell time used is still too short, so the welding is not maximized. Furthermore, microstructural observations were carried out in region b and region c from the results of macrostructural observations.

a

b

Fig. 9. Metallography of Al-Mg at dwell time 300 milliseconds: *a* – macrostructure; *b* – microstructure of area b; *c* – microstructure of area c

Fig. 9, *b* shows the microstructure observation in the weld center, where the stir zone is seen on the aluminum sheet. The weld bond between the two dissimilar materials appears to be partially bonded. However, the short dwell time parameter causes less heat input to the stir zone so that the structure formed is not clearly visible and is not fully bonded. Microstructural observations in the weld side area are shown in Fig. 9, *c*. The hook is formed pointing upwards because, during the idle time process, the rotating pins tear the material on the bottom, moving up towards the material on the top sheet. Hook formation or partial metallurgy is generally caused by tearing and breaking of the oxide layer at the interface between two sheets of discontinuous material particles that form the hook [25].

Metallographic observations at a dwell time of 500 milliseconds and a plunge depth of 600 microns are shown in Fig. 10. Macro structurally, a relatively low flash formation can be seen in Fig. 10, *a*. The joint between the two dissimilar materials appears to be well-related macro structurally. Region b and area c in the observation of the macrostructure will be further observed. Region b is located in the middle of the weld (Fig. 10, *b*), while region c is located on the side of

the weld (Fig. 10, *c*). Based on microstructural observations in the center of the weld, it can be seen that the tool penetrates the magnesium material so that the pin diameter causes the aluminum material to run out. In addition, the stir zone is seen on the magnesium sheet with large grains. This excessive depth is caused because the dwell time used is long enough so that the heat input that occurs is relatively high. This causes the aluminum material to run out on the tool pin diameter.

Furthermore, on the side of the weld, a hook is formed in an upward direction. The stir zone can also occur on aluminum sheets and TMAZ on magnesium sheets in this region. The grain size seen in aluminum is smaller than in magnesium. The region of intermetallic compounds (IMC) was also observed to be thin between the two materials. IMC that appears at the interface of magnesium and aluminum alloys [21].

Fig. 11 shows the results of metallographic observations carried out at a dwell time of 700 milliseconds and a plunge depth of 600 microns. Based on the results of macrostructural observations (Fig. 11, *a*), it can be seen that flash occurs in the side region of the weld. In addition, it is also seen that the aluminum sheet on the side is also lifted up so that the displacement is relatively high. This happens because the dwell time used is very long, causing an increase in heat input between the tool and the workpiece. Due to the heat, the area next to the weld will also be lifted up. The b and c regions of the macrostructural observations were further investigated in Fig. 11, *b*, *c*, respectively.

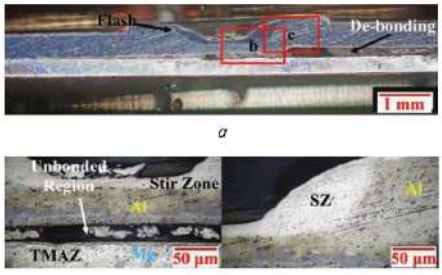

Fig. 10. Metallography of Al-Mg at dwell time 500 milliseconds: *a* — macrostructure; *b* — microstructure of area b; *c* — microstructure of area c

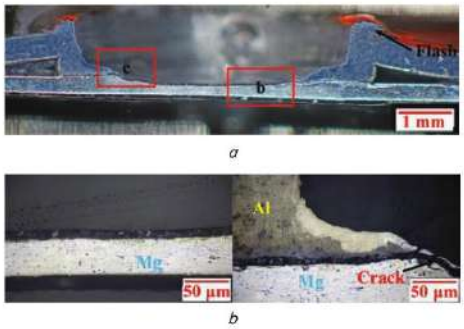

Fig. 11. Metallography of Al-Mg at dwell time 700 milliseconds: *a* — macrostructure; *b* — microstructure of area b; *c* — microstructure of area c

Microstructural observations show a fracture in the stir zone in the center of the weld. The cracks are straight along the stir zone, but there are no cracks in the magnesium sheet. Meanwhile, there are also quite large cracks in the area beside the weld. The observed IMC between the two materials is quite visible, with a fairly strong bond in the middle region of the weld. However, on the side of the weld, the bond is less than perfect due to the cracks that occur. This is because the tool stirs the workpiece for too long, causing cracks to occur in the aluminum sheet. The heat input and grain size in the stir zone are affected by the dwell time of the AZ31 magnesium alloy [26].

6. Discussion of the experimental results of the variation parameter micro-Friction Stir Spot Welding for weld geometry, mechanical properties and metallography

The weld shape is checked by measuring the diameter of the weld nugget, which consists of the shoulder diameter and pin diameter. Diameter measurements were carried out using Dino-Lite. Measurements are made at the top and back of the weld. This method has also been used by researchers in previons research on orbital pipe welding [27]. At the top of the plate, it can be seen visually that the shoulder diameter begins to form at a plunge depth of 400 microns and increases at a plunge depth of 600 microns. Mixing time also affects the size of the diameter of the formed shoulder. The two materials were stirred for a long time, increasing heat [10]. The friction between the shoulder and the material creates the weld nugget. Area measurements were carried out on the backside of the plate to see how large the TMAZ area was formed due to changes in dwell time and plunge depth. The deeper the tool is used, the larger the TMAZ area at the back of the plate [24].

The weld shape in the form of pin diameter tends to increase with increasing plunge depth and dwell time. The pin diameter measured is close to the diameter of the pin tool used. The longer the welding process, the more heat is generated and the larger the diameter of the welding pin [22]. The measured shoulder diameter is still below the tool shoulder pin diameter. This is due to the effect of the depth of the seam used. Due to the shallow depth of the plunge, the pin shoulder diameter does not rub completely against the material [13]. Therefore, the diameter of the weld shoulder is smaller and vice versa. The seam depth measured against the seam depth set by the tool makes a difference, especially with a downtime of 300 ms. Due to the dwell time of 300 ms, the heat generated by the friction between the tool and the specimen is insufficient, and the weld depth is not optimal. In contrast to a hold time of 700 ms, this hold time results in longer friction and maximum weld depth, resulting in higher heat absorption of the specimen. In addition, the area of the TMAZ is affected by the plunge depth and dwell time, where these two parameters have a straight ratio to the area of the TMAZ. The longer the friction between the tool and the test object, the greater the heat that will occur, causing the TMAZ area to be larger [1]. A deeper depth of plunge also supports this.

The tensile test provides maximum shear load and maximum cross load. Increasing the penetration depth can increase the maximum tensile strength and increasing the dwell time can also increase the maximum tensile strength of the weld. FSSW parameters such as dwell time and pen-

etration depth affect the maximum tensile strength. As the depth of the plunge increases, so does the joint between the two specimens, depending on the plate and the thickness of the tool used. In this case, the friction between the tool and the specimen has a longer effect on heating and thus on the quality of the weld joint [22]. Dwell time affects the increase in tensile strength [24]. In another study using pipe material with the FSW method [28], adding friction time to a certain value can increase its tensile strength.

The plunge depth phenomenon, which has unique properties mentioned in macrostructural analysis, helps to explain hook formation. It was also previously explained that the hook formation is closely related to the hook formation. Material flow, i. e., spotting during welding. Hooks are also associated with strength. Therefore, it can be discussed in detail about the ultrastructure of each existing tool to find out why this phenomenon occurs. For embedded tools based on the journal [26] and the researcher assumed that there was a maximum weld seam strength [24]. A schematic of the formation of the hook and extrude zone on the plate can be seen in Fig. 12. The shape of the tool with pins produces a strength that varies with the value of the height of the tool. If the height of the tool shape pin is X, then the X+Y depth results in the maximum weld strength. This is one of the Y variables, the maximum strength threshold depth, which can be used to further investigate the maximum strength value for the tool shape with pins or other shapes.

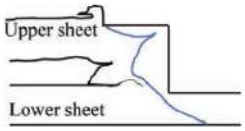

Fig. 12. The schematic of the formation of the hook and extrude zone on the plate [10]

The application of μFSSW welding has been widely applied in several industries, for example the automotive industry in the manufacture of vehicle cabins and bodies. Applications of different materials have also been widely applied. However, if this research is applied in practice, it still has some limitations. These limitations include the need for μFSSW mechanism that is smaller and difficult to use in a narrow space. However, the μFSSW method is very promising to produce better weld quality for different materials with thickness <1 mm.

In this research, no numerical/simulation studies have been conducted. Simulation studies need to be carried out to determine the initial characteristics of several variations of the μFSSW parameter. In addition, this study also has not analyzed the distribution of temperature and axial force that occurs during the welding process. This can actually be done with a simulation study that can be done before taking experimental data. Research development that can still be developed further is to compare the results of simulation studies and experiments on the distribution of temperature, axial force and weld geometry formed after the welding process. This research is one of the opportunities that can be done in further research.

7. Conclusions

1. The weld geometry formed in μFSSW is influenced by dwell time and plunge depth, where at a dwell time of 700 milliseconds and a plunge depth of 600 microns the weld pin diameter and weld shoulder diameter are close to the pin diameter and the diameter of the shoulder tool used.

2. Maximum shear load and cross load are strongly influenced by dwell time and plunge depth. The maximum shear load reached 387±17 N at a dwell time of 700 milliseconds and a plunge depth of 500 microns, while the dwell time of 700 milliseconds and a plunge depth of 600 microns produced the largest maximum cross load of 29±2 N.

3. Macrostructural observations show that there is a thin flash at the weld edge while a layer of intermetallic compounds is observed at the interface of the two materials. In addition, a dwell time of 700 milliseconds gives the effect of cracks on the inside of the weld.

Conflict of interest

The authors declare that they have no conflict of interest in relation to this research, whether financial, personal, authorship or otherwise, that could affect the research and its results presented in this paper.

Acknowledgments

This research is supported by the Automation and Manufacturing Systems laboratory, Department of Mechanical Engineering, Faculty of Engineering, Universitas Indonesia.

References

1. Mohammadi, J., Behnamian, Y., Mostafaei, A., Izadi, H., Saeid, T., Kokabi, A. H., Gerlich, A. P. (2015). Friction stir welding joint of dissimilar materials between AZ31B magnesium and 6061 aluminum alloys: Microstructure studies and mechanical characterizations. Materials Characterization, 101, 189–207. doi: https://doi.org/10.1016/j.matchar.2015.01.008
2. Lee, C.-Y., Lee, W.-B., Kim, J.-W., Choi, D.-H., Yeon, Y.-M., Jung, S.-B. (2008). Lap joint properties of FSWed dissimilar formed 5052 Al and 6061 Al alloys with different thickness. Journal of Materials Science, 43 (9), 3296–3304. doi: https://doi.org/10.1007/s10853-008-2525-1
3. Liu, L., Wang, H., Song, G., Ye, J. (2006). Microstructure characteristics and mechanical properties of laser weld bonding of magnesium alloy to aluminum alloy. Journal of Materials Science, 42 (2), 565–572. doi: https://doi.org/10.1007/s10853-006-1068-6
4. Huang, Y., Meng, X., Zhang, Y., Cao, J., Feng, J. (2017). Micro friction stir welding of ultra-thin Al-6061 sheets. Journal of Materials Processing Technology, 250, 313–319. doi: https://doi.org/10.1016/j.jmatprotec.2017.07.031
5. Nandan, R., Debroy, T., Bhadeshia, H. (2008). Recent advances in friction-stir welding – Process, weldment structure and properties. Progress in Materials Science, 53 (6), 980–1023. doi: https://doi.org/10.1016/j.pmatsci.2008.05.001

6. Song, Y., Yang, X., Cui, L., Hou, X., Shen, Z., Xu, Y. (2014). Defect features and mechanical properties of friction stir lap welded dissimilar AA2024–AA7075 aluminum alloy sheets. Materials & Design, 55, 9–18. doi: https://doi.org/10.1016/j.matdes.2013.09.062
7. Mishra, R. S., Ma, Z. Y. (2005). Friction stir welding and processing. Materials Science and Engineering: R: Reports, 50 (1-2), 1–78. doi: https://doi.org/10.1016/j.mser.2005.07.001
8. Rodrigues, D. M., Loureiro, A., Leitao, C., Leal, R. M., Chaparro, B. M., Vilaça, P. (2009). Influence of friction stir welding parameters on the microstructural and mechanical properties of AA 6016-T4 thin welds. Materials & Design, 30 (6), 1913–1921. doi: https://doi.org/10.1016/j.matdes.2008.09.016
9. Thomas, W., Nicholas, E. D., Staines, D., Tubby, P. J., Gittos, M. F. (2005). FSW Process Variants and Mechanical Properties. Welding in the World, 49 (3-4), 4–11. doi: https://doi.org/10.1007/bf03266468
10. Baskoro, A. S., Hadisiswojo, S., Kiswanto, G., Winarto, Amat, M. A., Chen, Z. W. (2019). Influence of welding parameters on macrostructural and thermomechanical properties in micro friction stir spot welded under high-speed tool rotation. The International Journal of Advanced Manufacturing Technology, 106 (1-2), 163–175. doi: https://doi.org/10.1007/s00170-019-04490-8
11. Darmadi, D. B., Abdillah, F. N., Raharjo, R. (2019). Controlling the pressure force to obtain a better quality of aluminum 6061 friction stir welded joint. Eastern-European Journal of Enterprise Technologies, 3 (1 (99)), 6–10. doi: https://doi.org/10.15587/1729-4061.2019.159286
12. Saeid, T., Abdollah-zadeh, A., Shibayanagi, T., Ikeuchi, K., Assadi, H. (2010). On the formation of grain structure during friction stir welding of duplex stainless steel. Materials Science and Engineering: A, 527 (24-25), 6484–6488. doi: https://doi.org/10.1016/j.msea.2010.07.011
13. Lin, Y.-C., Lin, J.-J., Lin, B.-Y., Lin, C.-M., Tsai, H.-L. (2012). Effects of process parameters on strength of Mg alloy AZ61 friction stir spot welds. Materials & Design, 35, 350–357. doi: https://doi.org/10.1016/j.matdes.2011.08.050
14. Avula, D., Singh, R. K. R., Dwivedi, D. K., Mehta, N. K. (2011). Effect of friction stir welding on microstructural and mechanical properties of copper alloy. World Academy of Science, Engineering and Technology, 50, 210–218. Available at: https://citeseerx.ist.psu.edu/viewdoc/download?doi=10.1.1.882.1571&rep=rep1&type=pdf
15. Gangwar, K., Ramulu, M. (2018). Friction stir welding of titanium alloys: A review. Materials & Design, 141, 230–255. doi: https://doi.org/10.1016/j.matdes.2017.12.033
16. Hussein, S. A., Tahir, A. S. M., Hadzley, A. B. (2015). Characteristics of aluminum-to-steel joint made by friction stir welding: A review. Materials Today Communications, 5, 32–49. doi: https://doi.org/10.1016/j.mtcomm.2015.09.004
17. Chen, Y. C., Nakata, K. (2010). Effect of surface states of steel on microstructure and mechanical properties of lap joints of magnesium alloy and steel by friction stir welding. Science and Technology of Welding and Joining, 15 (4), 293–298. doi: https://doi.org/10.1179/136217109x12568132624325
18. Li, G., Zhou, L., Zhou, W., Song, X., Huang, Y. (2019). Influence of dwell time on microstructure evolution and mechanical properties of dissimilar friction stir spot welded aluminum–copper metals. Journal of Materials Research and Technology, 8 (3), 2613–2624. doi: https://doi.org/10.1016/j.jmrt.2019.02.015
19. Esmaeili, A., Givi, M. K. B., Rajani, H. R. Z. (2011). A metallurgical and mechanical study on dissimilar Friction Stir welding of aluminum 1050 to brass ($CuZn_{30}$). Materials Science and Engineering: A, 528 (22-23), 7093–7102. doi: https://doi.org/10.1016/j.msea.2011.06.004
20. Salari, M. (2020). Dissimilar Friction Stir Welding between Magnesium and Aluminum Alloys. Journal of Modern Processes in Manufacturing and Production, 9 (3), 65–72. Available at: http://mpmpjournal.iaun.ac.ir/article_675991_70a99c7c7d6c3275c6c615bf68b17801.pdf
21. Chen, Y. C., Nakata, K. (2008). Friction stir lap joining aluminum and magnesium alloys. Scripta Materialia, 58 (6), 433–436. doi: https://doi.org/10.1016/j.scriptamat.2007.10.033
22. Kwon, Y. J., Shigematsu, I., Saito, N. (2008). Dissimilar friction stir welding between magnesium and aluminum alloys. Materials Letters, 62 (23), 3827–3829. doi: https://doi.org/10.1016/j.matlet.2008.04.080
23. Sen, M., Shankar, S., Chattopadhyaya, S. (2020). Micro-friction stir welding (μFSW) – A review. Materials Today: Proceedings, 27, 2469–2473. doi: https://doi.org/10.1016/j.matpr.2019.09.220
24. Sunar Baskoro, A., Azwar Amat, M., Andre Widiyanto, M. (2019). Effect of Tools Geometry and Dwell Time on Mechanical Properties and Macrograph of Two-Stage Refilled Friction Stir Spot Micro Weld. MATEC Web of Conferences, 269, 02002. doi: https://doi.org/10.1051/matecconf/201926902002
25. Badarinarayan, H., Yang, Q., Zhu, S. (2009). Effect of tool geometry on static strength of friction stir spot-welded aluminum alloy. International Journal of Machine Tools and Manufacture, 49 (2), 142–148. doi: https://doi.org/10.1016/j.ijmachtools.2008.09.004
26. Yang, X., Feng, W., Li, W., Dong, X., Xu, Y., Chu, Q., Yao, S. (2019). Microstructure and properties of probeless friction stir spot welding of AZ31 magnesium alloy joints. Transactions of Nonferrous Metals Society of China, 29 (11), 2300–2309. doi: https://doi.org/10.1016/s1003-6326(19)65136-8
27. Widyianto, A., Baskoro, A. S., Kiswanto, G., Ganeswara, M. F. G. (2021). Effect of welding sequence and welding current on distortion, mechanical properties and metallurgical observations of orbital pipe welding on SS 316L. Eastern-European Journal of Enterprise Technologies, 2 (12 (110)), 22–31. doi: https://doi.org/10.15587/1729-4061.2021.228161
28. Irawan, Y. S., Choiron, M. A., Suprapto, W. (2021). Tensile strength and thermal cycle analysis of AA6061 friction weld joints with different diameters and various friction times. Eastern-European Journal of Enterprise Technologies, 2 (12 (110)), 15–21. doi: https://doi.org/10.15587/1729-4061.2021.227224

2. Artikel 2 (Sudah dipresentasikan di ISAIME 2022)

Variation of Micro Friction Stir Spot Welding (μFSSW) Parameters on Metallography with Similar Materials AA1100

S. B. Membala[1,4], O. S. Sutresman[2], H. Arsyad[2*], M. Syahid[2] and A. Widyianto[3]

[1]Graduate Student in Mechanial Enginering Departement Hasanuddin University. Jl. Poros Malino KM.6 Bontomarannu Gowa, 92171, Sulawesi Selatan, Indonesia
[2]Departement of Mechanical Enginering Hasanuddin University. Jl. Poros Malino KM.6 Bontomarannu Gowa, 92171, Sulawesi Selatan, Indonesia
[3]Department of Automotive Engineering Education, Faculty of Engineering, Universitas Negeri Yogyakarta, Yogyakarta, Indonesia
[4]Department of Mechanical Enginering Cenderawasih University. Jl. Kampwolker, Kelurahan Yabansai, Distrik Heram, Jayapura-Papua, Indonesia

E-mail: arsyadhairul@yahoo.com

Abstract. The Micro Friction Stir Spot Welding (m-FSSW) process is a metal plate welding technique with a relatively thin plate thickness. The advantages of this welding are the higher quality of the weld and the relatively low deformation. This study aimed to determine the effect of depth of penetration, dwell time, and tool geometry on the trend of material flow on the macrostructure of the welds produced in the Micro Stir Spot Welding (m-FSSW) technique using AA1100 thin aluminum plates. In this study, the parameters that are changed are the depth of the chisel, dwell time, and tool geometry. In this study, the parameters of the penetration depth were divided into 500 microns, dwell time was split into three lengths of time (300 ms, 500 ms, and 700 ms), and tool geometry was divided into two types of tool geometries (tool-1 and tool-2). In addition, the macro test was carried out to determine the depth of the weld, contour profile, and stretch macrostructure. The results of the macro test will be used to analyze the material flow relationship in each weld zone on the welding results of all existing parameters. Based on the results of the study, the effect of depth of penetration, dwell time, and tool geometry on the weld depth and metallography (hook width, hook height, and effective top sheet thickness) of welds using AA1100 thin plates is influential along with various tool geometries and the deeper the weld penetration and the longer stirring time, although the results are not always directly proportional.

Keywords: Micro Friction Stir Spot Welding, Aluminum, Metallography, Similar material

1. Introduction

Welding is a process of joining material with another material by heating the material to the welding temperature, with or without a change in pressure, and with or without the use of filler material or filler [1]. 1991 was the year of the discovery of one type of welding technique that utilizes heat from friction called Friction Stir Welding (FSW), which was discovered by The Welding Institute (TWI) in the United Kingdom [2, 3]. This FSW is suitable for application to aluminum materials. Friction Stir Spot Welding is a branch of Friction Stir Welding. Friction Stir Spot Welding (FSSW) is a welding

technique in the Solid-State phase. FSSW in the stabbing process, uses a rotating chisel with a protruding pin geometry.

Conceptually, Micro Friction Stir Spot Welding (μFSSW) is very similar to the FSSW method, which differs only in the thickness of the material. FSSW is intended for materials whose thickness is less than 1 mm. Due to the penetration between the tool and the overlapping material, there is heat that causes the material to soften and coalesce, causing a joint in the weld zone. There are two types of connections in the FSSW method: complete metallurgical bonds and partially metallurgical bonds [4]. From the weld zone formed there is also the term "hook". This hook is a term for partial metallurgical bond [5], this hook can also be interpreted as a weld defect caused by the effect of tool stirring and creases in the FSSW weld zone. This hook is also one of the parameters of the success of a weld.

Yin, Y.H. et al. [6] have investigated the hook formation and mechanical properties of the AZ31 material in the Stir Spot Welding welding technique. Baskoro et al. [7] have also investigated the effect of HSS-based tools on the mechanical properties of welds using Response Surface Methods (RSM) with AA1100 Aluminum material. High Strength Steel is a type of material that can be used as a welding tool with the FSSW method. The tool geometry and the stitch's depth variation are important parameters in the FSSW process. Research on the effect of weld geometry and variations of puncture depth on μFSSW with AA5052 material on welds' mechanical properties and geometry has been carried out by Zhang et al. [8]. A similar study on the effect of the diameter width, and depth of the chisel (flat chisel or probeless tools) on μFSSW on AA1100 material on the mechanical properties and joint width has also been carried out by Baskoro et al [9]. Research on welding parameters has been carried out by A. S. Baskoro [9] as mentioned above regarding the effect of welding parameters and rotational speed of the tool in the μFSSW process using A1100 aluminum.

Boz and Kurt [10] investigated the relationship between tool geometry and mechanical properties in FSW processes. Next, Zhang et al. [8] investigated the effect of welding parameters on temperature and material behavior in the FSW process. As a result, it was found that increasing the number of turns and decreasing the welding speed in tool welding increased the stirring effect and improved the quality of the FSW. Finally, Tran et al. [11] studied the effect of machining time on strength and failure models of two different types of FSSW between 5754-O and 7075-T6 aluminum plates. Their test results showed that both types of welds failed with longer processing times.

The tool geometry greatly affects the input energy, deformation pattern, puncture force, microstructure, and mechanical properties of the FSW joint. Rai et al. [12] reviewed and investigated several key aspects of FSW tools, including the tool selection process, geometry and toughness, tool degradation mechanisms, and process costs. Buffa et al. [13] studied the FSW process of aluminum alloys using the model developed by the authors. The research carried out in this paper describes the FSW process at different depths. The most important geometric parameter in the FSW tool design is the shoulder diameter, which is still being developed by trial and error.

Departing from the previous problem, further investigation of the defects in the weld results and regarding the material flow process in AA1100 thin plate welding is necessary. The thickness of the AA1100 plate is 0.32 mm and is joined by spot welding. Hence, the variation of μFSSW parameters such as penetration depth, dwell time, and tool geometry. After the welding process is complete, metallographic testing is carried out to determine the quality of the weld.

2. Experiment Method

This study uses a material similar to aluminum AA100 with micro-friction stir spot welding (μFSSW) with a thickness of 0.32. Testing of the chemical composition of the AA100 material was carried out using an optical emission spectrometer (OES), and the results are shown in Table 1. Before welding, both materials were cleaned with acetone to remove residual dirt and dust on the panel surface.

Table 1. Chemical composition (wt %) of AA1100

	Al	Zn	Mn	Fe	Si	Cu	Ti	Mg
AA1100	99.1	0.070	0.043	0.471	0.109	0.057	0.012	0.019

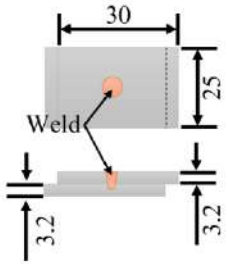

Figure 1. Metallographic test specimen dimensions

The welding used is μFSSW spot welding. Samples were prepared for triplicate metallographic examination. The dimensions of the metallographic specimen shown in Figure 1 are 30 mm long and 25 mm wide. The dimensions of the tools used for the μFSSW are shown in Figure 2. Two types of tools were used: pin 600 (Figure 2a) and two-stage shoulders (Figure 2b). The tool material used is high-speed steel (HSS) which is made by turning the machine. The stir point friction welding tool in this study uses a modified EMCO CNC TU-3A milling machine tensile tester with an accuracy of 0.01 mm. While the spindle used is a Mactec MT912 rotary drill with a die grinder specification of 6 mm and a spindle speed of 33,000 rpm. Table 2 shows the parameters of the μFSSW welding process used in this study.

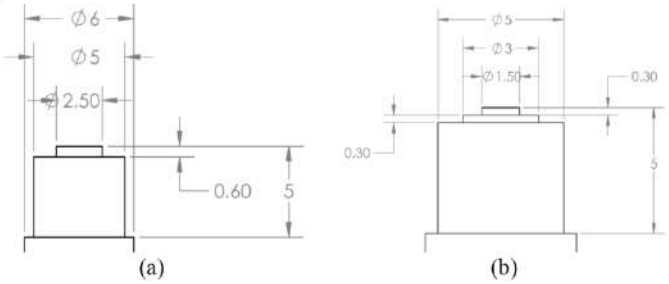

Figure 2. Tool dimensions of (a) pin 600 and (b) two-stage shoulder

Table 2. Parameters process of μFSSW

No.	Plunge rate (mm/s)	Plunge depth (microns)	Tool	Dwell time (milliseconds)
1	0.4	400	Tool 1	300
2				500
3				700
4			Tool 2	300
5				500
6				700

Metallographic examinations carried out included the macrostructure and microstructure of the weld. The sample is cut and then subjected to metallographic preparation including grinding, polishing, and etching. In addition, the macrostructure was observed with a digital microscope (Dino-Lite AM 4115 series) and the microstructure with an optical microscope (Oxion Inverso OX 2153-PLM).

3. Results and Discussion

3.1. Macrostructure

Macrostructure testing was conducted to determine the width and height of the hook formed, the direction of the hook formed, and the effective thickness of the top sheet of the weld. Meanwhile, microstructure testing was carried out to determine the boundaries between the µFSSW welded areas.

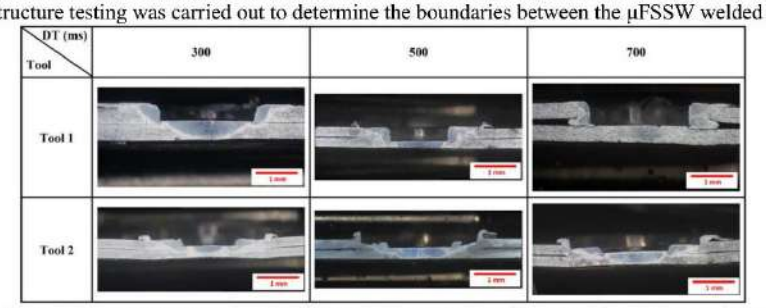

Figure 3. Macrostructure with Al-Al material in several variations of dwell time and tools

Figure 3 shows the results of observing the macrostructure with Al-Al material in several variations of dwell time and tool geometry. It can be seen that the geometry of the tools affects the material flow of the aluminum material. At the same time, the diameter of the weld will be wider if the stirring time is prolonged. Visually it can be seen that it produces a fairly good weld at a dwell time of 500 ms. Flash also appears at the edges of the weld for all variations of welding parameters. The effect of shoulder diameter on thermal cycling, peak temperature, power, and torque on the FSW process is very complex and needs further study. The criteria of the tool design process for the shoulder diameter based on the principle of maximum torque for traction have been proposed and tested [13].

3.2. Microstructure

Microstructural observations were carried out on various parameters of µFSSW, namely dwell time and tool geometry. While the plunge depth used is constant at 500 microns. Microstructural observations in the center of the weld and the weld edges on the left and right sides. The things that were observed were changes in structure, flash, hook formed and cracks.

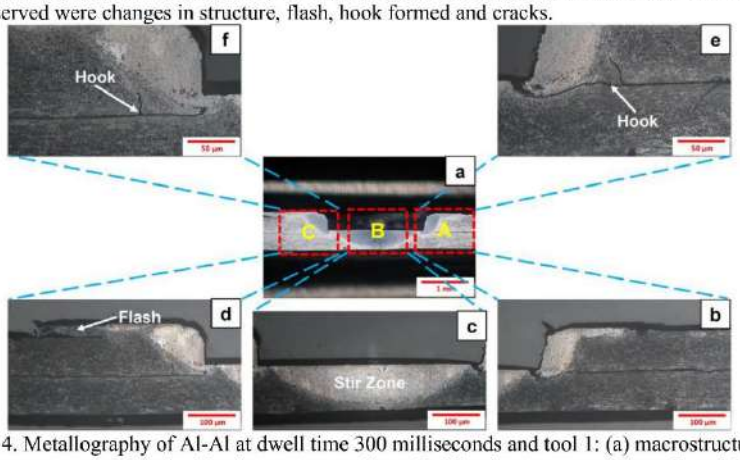

Figure 4. Metallography of Al-Al at dwell time 300 milliseconds and tool 1: (a) macrostructure, (b) microstructure of area A, (c) microstructure of area B, (d) microstructure of area C, and (e, f) microstructure with high magnification

Figure 4 shows the results of the macro and microstructure of Al-Al material at the dwell time parameter of 300 ms and tool 1. Welding defects in the form of flash began to appear on the left edge

of the weld. The plunge depth used is constant, which is 500 microns. From the macro structure, the stir zone (SZ) area and the penetration depth (see Figure 4a) can be seen. A dwell time of 300 ms is the lowest parameter. This causes the heat generated also tends to be lower. Area A is further observed in the microstructure shown in Figure 4b. Area A is the weld area on the right side, where on the right side, no flash is formed. Area B is the SZ area which is right in the middle, as shown in Figure 4c. Based on the micro results, it can be seen that the two materials can be connected perfectly. Area C is the weld area on the left side, where flash appears, as shown in Figure 4d. Areas A and C are the sides of the weld, where extend or flash areas appear. The flow transition zone (FTZ) is observed at the edge of the weld, where friction occurs between the material and the shoulder pin tool. Furthermore, the stir zone (SZ) is also visible on the surface of the weld that rubs against the surrounding surface of the tool pin. If areas A and C are enlarged again, it can be seen that the hook formed on the side of the weld (see Figure 4 e,f).

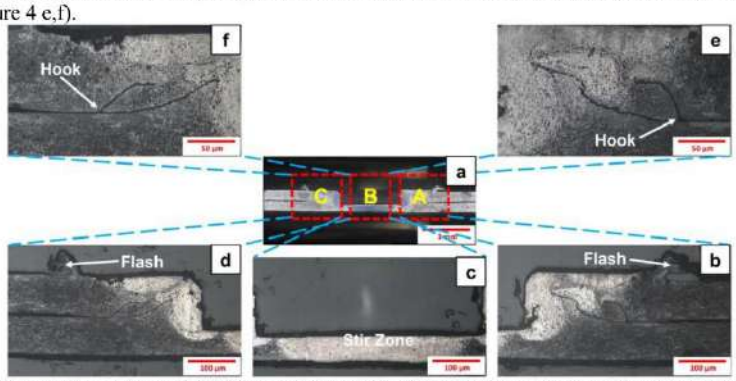

Figure 5. Metallography of Al-Al at dwell time 500 milliseconds and tool 1: (a) macrostructure, (b) microstructure of area A, (c) microstructure of area B, (d) microstructure of area C, and (e, f) microstructure with high magnification

Figure 5a shows the results of macro-structure observations for Al-Al material with a dwell time parameter of 500 ms and tool 1. The flash created on the upper plate is quite high, but some areas are not perfectly bonded. Microstructure observations were made in areas A and C, as shown in Figures 5b and 5d. In the middle area of the weld, you can see the rest of the upper plate which is attached to the lower plate due to friction with the tool. The SZ and TMAZ regions are visible on the bottom plate. Figure 5c shows the results of microstructure observations in area B. The hook formed tends to point upwards, and there are a few cracks on the left and right sides of the weld (see Figures 5e and 5f).

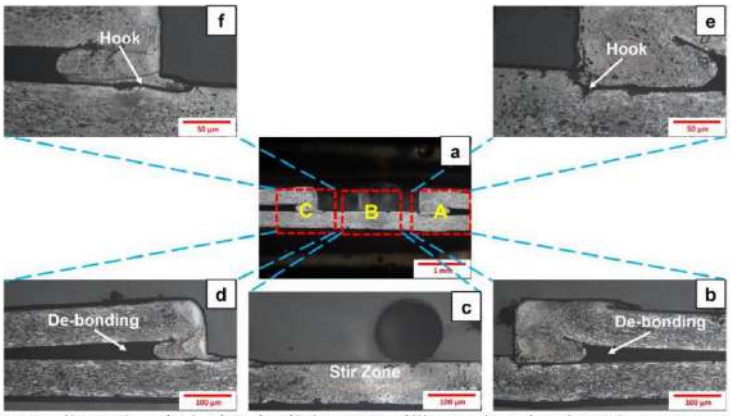

Figure 6. Metallography of Al-Al at dwell time 700 milliseconds and tool 1: (a) macrostructure, (b) microstructure of area A, (c) microstructure of area B, (d) microstructure of area C, and (e, f) microstructure with high magnification

Furthermore, macro-structural observations were carried out on Al-Al material with a dwell time parameter of 700 ms and tool-1, as shown in Figure 6a. The side area of the weld is not properly bonded because the top plate is lifted. The longer the stirring time occurs, the top plate can be lifted up in the area that is not exposed to the tool. The next observation is the microstructure in the middle area of the weld (area B) which is shown in Figure 6c. Based on these observations, the SZ, TZ and TMAZ areas on the bottom plate can be seen. The top plate blends with the bottom plate perfectly in the middle. The areas A and C, which are the weld edges of the right and left sides are observed in the microstructure and are shown in Figures 6b and 6d. Based on the figure, it can be seen that there is an area that is not well bound, which is next to SZ. The EXTD region was also observed in the non-bound region of the upper plate. While the flash formed is relatively lower. Figures 6e and 6f are high magnifications of the weld edge area on the left and right sides. In this picture you can see the direction of the hook formed from the welding results.

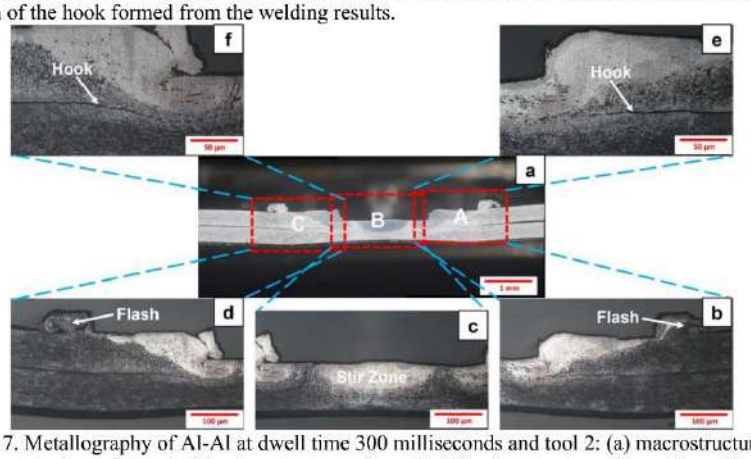

Figure 7. Metallography of Al-Al at dwell time 300 milliseconds and tool 2: (a) macrostructure, (b) microstructure of area A, (c) microstructure of area B, (d) microstructure of area C, and (e, f) microstructure with high magnification

Figure 7a shows the results of the macrostructure of the Al-Al material at the dwell time parameter of 300 ms and tool 2. Welding defects in the form of flash began to appear on the right and

left edges of the weld. The depth of the puncture looks very shallow because the dwell time used is the lowest. This causes the heat generated to be lower and the weld penetration to become shallow. Area B is further observed in the microstructure shown in Figure 7c. Area B is the SZ area which is right in the middle. Based on the micro results, it can be seen that the two materials can be connected perfectly. The SZ region on the top plate and the TMAZ region on the bottom plate can be clearly observed. Figures 7b and 7d show the microstructure results in areas A and C. Areas A and C are the sides of the weld on the right and left sides, where extend or flash areas appear. The flow transition zone (FTZ) is observed at the edge of the weld, where friction occurs between the material and the shoulder pin tool.

Furthermore, the stir zone (SZ) is also visible on the surface of the weld that rubs against the surrounding surface of the tool pin. The hook formed leads to the bottom plate, as shown in Figures 7e and 7f. The relatively short stirring time causes the hook formed to point downwards.

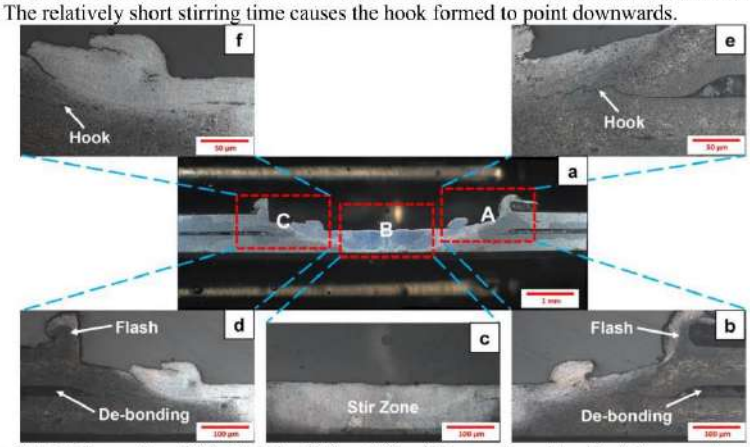

Figure 8. Metallography of Al-Al at dwell time 500 milliseconds and tool 2: (a) macrostructure, (b) microstructure of area A, (c) microstructure of area B, (d) microstructure of area C, and (e, f) microstructure with high magnification

Figure 8a shows the results of observing the macrostructure of the Al-Al material at the dwell time parameter of 500 ms and tool 2. The unbound area between plates is visible on the right and left sides of the weld. The flash that is formed is also quite high. This is because the tool's geometry has two stage shoulders with a long dwell time that causes the top plate to lift. Area B is further observed in the microstructure observations shown in Figure 8c. SZ, TZ, and TMAZ regions appear on the bottom plate. Furthermore, microstructure observations were carried out again in areas A and C as shown in Figures 8b and 8d. A slight crack beside the hook forms on the left side of the weld as shown in Figures 8e and 8f. The difference in microstructure can be seen from the area that rubs against the tool and the base metal.

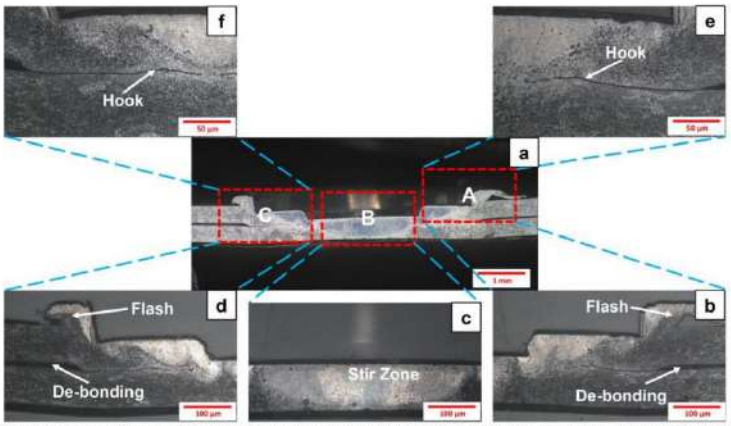

Figure 9. Metallography of Al-Al at dwell time 700 milliseconds and tool 2: (a) macrostructure, (b) microstructure of area A, (c) microstructure of area B, (d) microstructure of area C, and (e, f) microstructure with high magnification

Figure 9a shows the results of macro-structure observations on Al-Al material with dwell time parameters of 700 ms and tool 2. The side of the weld on the top plate is raised quite high and causes the area not to be appropriately bonded. This happens because the dwell time used is the highest, so the heat is higher and presses the top plate. So that the top plate that is not exposed to the tool will be lifted, but it also forms a flash. Microstructure observations in area B have been carried out; the results are shown in Figure 9c. The SZ and TZ regions can be seen on the bottom plate. The heat-affected area looks different in its microstructure. Then the left and right weld edge areas (areas A and C) were further observed for their microstructure and shown in Figures 9b and 9d. The EXTD, FTZ, SZ and TZ regions can be observed at the edges of the weld. The flash that is formed can be seen clearly due to friction with the tool. The hook formed on the weld side tends to point upwards, as shown in Figures 9e and 9f.

Based on the observation of the microstructure for all welding parameters, it can be seen that a flash appears on the edges of the weld. This is because some samples' top plate on the side of the weld is not properly bonded. The trend obtained from the macrostructural search results regarding the value of the hook width tends to decrease slightly from the weld results with a dwell time of 300 ms, then drastically increases the hook width in the weld results with a dwell time of 500 ms and 700 ms. This is in accordance with the literature written by Badarinarayan et al. [5], which states that the longer the stirring time, the wider the hook width and leads to the top. The value of the hook height starting from the end of the metallurgical connection or perfect connection to the point between the two materials is also decreasing. This is also in accordance with the existing literature. When viewed from the hook's direction, the weld hook with 500 ms turns towards the upper material or towards the stirring zone.

4. Conclusions

This study completed the variation of Micro Friction Stir Spot Welding (μFSSW) welding parameters for AA1100-like materials. FSSW parameters include tool geometry (pin 600 and two-stage shoulder) and dwell time (300 ms, 500 ms, and 700 ms). The tool rotates at high speed of about 33,000 rpm and then presses the two materials. Based on the results of the study, the effect of dwell time and tool geometry on weld depth and metallography (hook width, hook height, and effective cover plate thickness) for welds using AA1100 sheet and various tool geometries and Weld depth results are not always directly proportional but increase penetration and stir time. At the same time, the diameter of the weld will be wider if the stirring time is prolonged. Visually, it produces a fairly good weld at a dwell time of 500 ms. Based on the observation of the microstructure for all welding parameters, the trend of the hook width values obtained from the microstructure search results shows a trend towards a

slight decrease at a dwell time of 300 ms and a significant increase in the hook width of the weld results at dwell times of 500 ms and 700 ms.

Acknowledgments
This research is supported by the Automation and Manufacturing Systems Laboratory, Department of Mechanical Engineering, Faculty of Engineering, Universitas Indonesia.

References

[1] J. G. Feldstein, "Welding and brazing qualifications," *ASME Boil. Press. Vessel Code,* vol. 2, pp. 189-225, 2002.
[2] W. M. Thomas, E. D. Nicholas, J. C. Needham, M. G. Murch, P. Templesmith, and C. J. Dawes, "Friction stir welding. International Patent Application No. PCT/GB92/02203 and GB Patent Application No. 9125978.8," *US Patent,* no. 5, pp. 460-317, 1991.
[3] W. M. Thomas and E. D. Nicholas, "Friction stir welding for the transportation industries," *Materials & design,* vol. 18, no. 4-6, pp. 269-273, 1997.
[4] H. Badarinarayan, Q. Yang, and S. Zhu, "Effect of tool geometry on static strength of friction stir spot-welded aluminum alloy," *International Journal of Machine Tools and Manufacture,* vol. 49, no. 2, pp. 142-148, 2009.
[5] H. Badarinarayan, Y. Shi, X. Li, and K. Okamoto, "Effect of tool geometry on hook formation and static strength of friction stir spot welded aluminum 5754-O sheets," *International Journal of Machine Tools and Manufacture,* vol. 49, no. 11, pp. 814-823, 2009.
[6] Y. H. Yin, N. Sun, T. H. North, and S. S. Hu, "Hook formation and mechanical properties in AZ31 friction stir spot welds," *Journal of Materials Processing Technology,* vol. 210, no. 14, pp. 2062-2070, 2010.
[7] A. S. Baskoro, G. Kiswanto, and W. Winarto, "Effects of high speed tool rotation in micro friction stir spot welding of aluminum A1100," vol. 493, pp. 739-742: Trans Tech Publ.
[8] Z. Zhang, X. Yang, J. Zhang, G. Zhou, X. Xu, and B. Zou, "Effect of welding parameters on microstructure and mechanical properties of friction stir spot welded 5052 aluminum alloy," *Materials & Design,* vol. 32, no. 8-9, pp. 4461-4470, 2011.
[9] A. S. Baskoro, A. Riyanto, M. F. Arifardi, and P. Rupajati, "Influence of Tools Diameters and Plunge Depth on Mechanical Properties of Micro Friction Stir Spot Welding Materials A1100," vol. 727, p. 012008: IOP Publishing.
[10] M. Boz and A. Kurt, "The influence of stirrer geometry on bonding and mechanical properties in friction stir welding process," *Materials & Design,* vol. 25, no. 4, pp. 343-347, 2004.
[11] V. X. Tran, J. Pan, and T. Pan, "Effects of processing time on strengths and failure modes of dissimilar spot friction welds between aluminum 5754-O and 7075-T6 sheets," *Journal of materials processing technology,* vol. 209, no. 8, pp. 3724-3739, 2009.
[12] R. Rai, A. De, H. Bhadeshia, and T. DebRoy, "friction stir welding tools," *Science and Technology of welding and Joining,* vol. 16, no. 4, pp. 325-342, 2011.
[13] A. Arora, A. De, and T. DebRoy, "Toward optimum friction stir welding tool shoulder diameter," *Scripta materialia,* vol. 64, no. 1, pp. 9-12, 2011.

[10] B. M. Semuel, S. S. Onny, A. Hairul, S. Muhammad, and W. Agus, "Indentifying the effect of micro friction stir spot welding (μFSSW) parameters on weld geometry, mechanical properties, and metallography on dissimilar materials of AZ31B and AA1100," *Eastern-European Journal of Enterprise Technologies,* vol. 4, no. 12 (118), pp. 13-21, 2022.

[11] V. Sanchez-Tembleque, V. Vedia, L. M. Fraile, S. Ritt, and J. M. Udias, "Optimizing time-pickup algorithms in radiation detectors with a Genetic algorithm," *Nuclear Instruments and Methods in Physics Research Section A: Accelerators, Spectrometers, Detectors and Associated Equipment,* vol. 927, pp. 54-62, 2019.

[12] X.-L. Luo, J. Feng, and H.-H. Zhang, "A Genetic algorithm for astroparticle physics studies," *Computer Physics Communications,* vol. 250, p. 106818, 2020.

[13] G. Senthilkumar and R. Ramakrishnan, "Design of Optimal Parameter for Solid-State Welding of EN 10028-P355 GH Steel Using gray Incidence Reinforced Response Surface Methodology," *Arabian Journal for Science and Engineering,* vol. 46, no. 3, pp. 2613-2628, 2021.

[14] A. S. Baskoro, A. Riyanto, M. F. Arifardi, and P. Rupajati, "Influence of Tools Diameters and Plunge Depth on Mechanical Properties of Micro Friction Stir Spot Welding Materials A1100," vol. 727, p. 012008: IOP Publishing.